

THESIS

ESTIMATES OF SUBLIMATION IN THE
UPPER COLORADO RIVER BASIN

Submitted by

Morgan Phillips

Department of Atmospheric Science

In partial fulfillment of the requirements

For the Degree of Master of Science

Colorado State University

Fort Collins, Colorado

Fall 2013

Master's Committee:

Advisor: William Cotton

John Stednick

Russ Schumacher

ABSTRACT

ESTIMATES OF SUBLIMATION IN THE UPPER COLORADO RIVER BASIN

Snowpack stored in mountain environments is the primary source of water for the population of much of the western United States, and the loss of water through direct evaporation (sublimation) is a significant factor in the amount of runoff realized from snow melt. A land surface modeling study was carried out in order to quantify the temporal and spatial variability of sublimation over the Upper Colorado River basin through the use of a spatially distributed snow-evolution model known as SnowModel. Simulations relied on forcing from high resolution atmospheric analysis data from the North American Land Data Assimilation System (NLDAS). These data were used to simulate snow sublimation for several years over a 400 by 400 km domain in the Upper Colorado River Basin at a horizontal resolution of 250 m and hourly time-steps.

Results show that total volume of sublimated water from snow varies 68% or between 0.95×10^7 acre feet in WY 2002 to the maximum of 1.37×10^7 acre feet in WY 2005 within the ten years of the study period. On daily timescales sublimation was found to be episodic in nature, with short periods of enhanced sublimation followed by several days of relatively low snowpack water loss. The greatest sublimation rates of approximately 3 mm/day were found to occur in high elevation regions generally above tree line in conjunction with frequent windblown snow, while considerable contributions from canopy sublimation occurred at mid-elevations. Additional sensitivity runs accounting for reduced canopy leaf area index as a result of western pine beetle induced tree mortality were also carried out to test the models sensitivity to land

surface characteristics. Results from this comparison show a near linear decrease in domain total sublimation with reduced LAI. Model performance was somewhat satisfactory, with simulations underestimating precipitation and accumulated SWE, most likely due to biases in the precipitation forcing and errors in determining precipitation phase.

ACKNOWLEDGMENTS

Special thanks to Nolan Doesken for providing me with the opportunity to work on this project and give me direction to complete it. I am also very grateful to Glen Liston, who's unimaginable help allowed me to even attempt a project of this scale. I would like to thank my advisor, William Cotton, and committee members John Stednick and Russ Schumacher for providing their time to help me become a better scientist.

Thanks also to the Colorado State University Atmospheric Science Department faculty, students and staff, especially Wendy Ryan for her almost daily advice. Funding support for this project was provided by the NIDIS Upper Colorado River Basin pilot project grant #NA09OAR4320074, the Colorado Climate Center and the State of Colorado.

Finally, I would like to thank my friends and parents for supporting me through this experience.

TABLE OF CONTENTS

ABSTRACT	ii
ACKNOWLEDGMENTS	iv
TABLE OF CONTENTS	v
LIST OF TABLES	vii
LIST OF FIGURES	viii
CHAPTER 1 : INTRODUCTION	1
Literature Review	2
Goals and Objectives	4
CHAPTER 2 : METHODS	6
Study Domain	6
Model Description	9
Data Description	10
Model Configurations	12
Data Analysis	14
CHAPTER 3 : RESULTS	15
Model Results	15
Validation/Comparison with Precipitation Observations	22
Sensitivity Analysis	24

Canopy Sensitivity	24
CHAPTER 4 : DISCUSSION.....	27
Static Sublimation.....	27
Blowing Snow Sublimation	28
Canopy Sublimation.....	30
Temporal Variability.....	34
Spatial Variability	37
Additional Concerns	38
Model Performance.....	39
Precipitation Validation	39
SWE Validation	40
CHAPTER 5 : CONCLUSIONS	43
Future Considerations	44
REFERENCES	47
APPENDIX A.....	53
APPENDIX B.....	55
APPENDIX C.....	56

LIST OF TABLES

Table 1-1: Summary of previous sublimation estimates and observations

Table B-1: Equivalent land type classification for the National Land Cover Dataset and land cover types found in SnowModel

LIST OF FIGURES

- Figure 2.1: Location of study domain and NLDAS grid-points
- Figure 2.2: Land use types in the study domain derived from the 2006 National Land Cover Database (Fry et al., 2011)
- Figure 2.3: 30 year average (1979-2009) SWE accumulation for SNOTEL stations located in the UCRB
- Figure 2.4: Location of SNOTEL sites used for validation and comparison of model results
- Figure 2.5: 10 year average seasonal cycles of temperature, relative humidity, wind speed and accumulated precipitation over the water year for NLDAS grid points nearest 69 SNOTEL locations
- Figure 3.1: Annual Domain total sublimation by type from October 1, 2001 through September 30, 2011
- Figure 3.2: Domain total sublimation normalized by area
- Figure 3.3: 10 Year simulated average daily sublimation smoothed with a 5-day running mean and 10 year average simulated SWE at 69 select SNOTEL sites
- Figure 3.4: Average annual sublimation simulated from October 1, 2001 through September 30, 2011
- Figure 3.5: Average sublimation rate on days when sublimation occurred from October 1, 2001 through September 30, 2011
- Figure 3.6: 10 year average annual sublimation volume binned by elevation
- Figure 3.7: Area of study domain binned by elevation
- Figure 3.8: 10 year average annual sublimation per unit area binned by elevation

Figure 3.9: 10 year average of annual fraction of sublimated precipitation

Figure 3.10: Comparison of observed precipitation from 69 SNOTEL sites to model simulated precipitation

Figure 3.11: Comparison of observed SWE values at 69 SNOTEL sites to model simulated SWE values

Figure 3.12: Difference in simulated canopy sublimation between the control and a 30% reduction in LAI sensitivity run for WY 2004-2005

Figure 3.13: Percent reduction in LAI vs. percent reduction in total sublimation

Figure 4.1: Annual average wind speed from the NLDAS grid points nearest the 69 select SNOTEL sites

Figure A-1: Average annual simulated blowing snow sublimation from October 1, 2001 through September 30, 2011

Figure A-2: Average annual simulated canopy sublimation from October 1, 2001 through September 30, 2011

Figure A-3: Average annual simulated static surface sublimation from October 1, 2001 through September 30, 2011

Figure C-1: Comparison of model derived precipitation to observations at 69 select SNOTEL sites

Figure C-2: Comparison of model derived SWE values to observations at 69 select SNOTEL sites

CHAPTER 1 : INTRODUCTION

Throughout much of the western United States, water reserves stored in the form of mountain snowpack provide the primary source of water for the population, agriculture and many high and middle elevation ecosystems (Doesken et al., 1996). This is particularly true in the Upper Colorado River Basin where up to 70% of annual flow originates from snowmelt alone (Christensen et al., 2007). The Upper Colorado River Basin (UCRB) is home to the headwaters of the Colorado River, one of the largest river systems in the western US. Located in the Southwestern US in portions of Colorado, Utah, Arizona and Wyoming, this large mountain catchment covers an area of approximately 112,000 mi² including some of the highest portions of the Rocky Mountain cordillera of North America.

Annual discharge volume from the UCRB as measured at Lee's Ferry, Arizona varies greatly from year to year, ranging from a low of 3.8×10^6 acre-feet in 2002 to 22.2×10^6 acre-feet in 1984 (USBR). Seasonal runoff from this river system is heavily regulated due to the high demand for water from downstream users in California and Nevada, and to meet water export quotas for existing compacts. Irrigation makes up the majority of water use within the UCRB, comprising 67% of total consumptive use of UCRB runoff with the remainder of the water being utilized for municipal water systems, hydroelectric generation or trans-basin diversions (Bureau of Reclamation, 2012).

Literature Review

The ablation of mountain snow packs through sublimation is recognized as an important factor in the removal of water throughout the winter season in mid-latitude mountain regions (Beaty, 1975, Marks et al., 1992, Pomeroy et al., 1991, 1993, MacDonald et al., 2010,). Results from a number of these previous sublimation studies are summarized in Table 1-1. Here it can be seen that sublimation loss can account from anywhere from 10% to 60% of the total snowpack mass, and significantly impact the water balance of the region (Schultz et al., 2004). Extreme cases of sublimation have been shown to be very efficient at removing snowpack water, with losses of up to 90% of annual snowpack on preferred alpine crests (Strasser et al., 2008), and rates exceeding 8 mm/day (Avery et al., 1992).

Table 1-1: Summary of previous sublimation estimates and observations

Author	Type	Amount
Avery et al., 1992	Static	1.56 mm/day (max of 8.52 mm/day)
Harding et al., 1996	Canopy	4 mm in 36 hours
Hood et al., 1994	Static and blowing	15% annual precip.
Kattleman et al., 1991	Alpine	1-2 mm/day, 18% ann. Precip.
Lundberg et al., 1994	Canopy	0.3 mm/hr
Liston et al., 1998	Arctic, blowing only	22% of winter precipitation
MacDonald et al., 2010	Alpine	20-30% annual snowfal
Marks et al., 1992	Alpine	20% annual snowfall
Meiman and Grant et al., 1974	Forest/Alpine	40% annual precip. canopy, 60% annual precip. Alpine
Molotch et al., 2004	Canopy	0.41 (sub-canopy) - 0.71 (canopy) mm/day
Montesi et al., 2004	Canopy	20-30% annual snowfall
Schmidt et al., 1998	Canopy	20% annu. Snow, 0.52 mm/day
Schmidt et al., 1992	Total Sub.	46 mm annually
Schultz et al., 2004	Desert Alpine	44% Snowpack (3 mm/day)
Strasser et al., 2008	Total Sub.	10-90% annual precip

The magnitude of sublimation has been shown to vary widely across different land surface environments and elevation (Fassnacht, 2004, Montesi et al., 2004, Molotch et al., 2007, Strasser, 2008, Fassnacht, 2010). These changes can include variability in surface features such as vegetation (Liston et al., 1995, Hiemstra et al., 2002) and topography/slope aspect (Zhang et al., 2004), as well as different environmental variables like wind, solar insolation, temperature and precipitation regime (Hood et al., 1999). Additionally, sublimation has been shown to vary greatly within the seasonal and sub-seasonal timeframe, with large losses during the wintertime and the potential for small amounts of condensation onto the snow surface during spring and early summer (Martinelli, 1960, Hood, 1999).

Evaporation from snow is important because unlike the liquid phase, precipitation in the form of snow remains on the surface and exposes the water to the atmosphere for extended periods of time. Loss of water via sublimation has the potential to affect the timing and amount of runoff realized from a mountain snowpack. Quantifying the magnitude and variability of this process over complex terrain is important to fully understand the local water balance, but remains an area that has not been studied well within the UCRB. While numerous studies exist that attempt to quantify snow sublimation from either point measurements or distributed physical models, there has yet to be a detailed modeling study of sublimation over the entire UCRB.

Operational snow models exist that have attempted to examine sublimation on the continental scale (Carroll et al., 2006), but have relied on coarse ($> 1 \text{ km}^2$) resolution models which may neglect influences of subtle terrain features, vegetation interception or transport and redistribution of snow. The vast majority of physical models have placed emphasis on the spatial distribution of snow in the calculations of snowpack evolution while neglecting processes associated with blowing and saltating snow (Pomeroy et al., 1993, Liston et al., 2006). Other efforts to simulate snow evolution over large catchments have used coarse parameterizations of sub-grid processes such sublimation from blowing snow that are not explicitly simulated in the model (Bowling et al., 2003). Modeling studies that have incorporated 3-D transport and energy fluxes have been relegated to small catchments on the order of 1 to 10's of km^2 (Winstral et al., 2002, Liston et al., 2007, Strasser et al., 2008) that do not allow for the identification of large scale spatial gradients, and may include local phenomena that are not representative of regional characteristics.

Goals and Objectives

Concern about surface water supply reductions via sublimation were raised as part of the National Integrated Drought Information System (UCRB) drought early warning system pilot project. The purpose of this study is to investigate the process of sublimation throughout the UCRB in an attempt to quantify both the spatial and temporal variability of water loss from wintertime snowpack through the use of a physically-based snowpack evolution model known as SnowModel (Liston et al., 1995, 1998, 2002, 2006, 2007, 2008). Specific goals include

1. Identify past and current observational datasets and sublimation study results from research in and near the UCRB
2. Assess data requirements and availability needed for estimating sublimation

3. Determine the optimal methodologies and data sets for estimating sublimation over a large area of complex topography
4. Using results from objectives 1-3, compute regional estimates of sublimation over various time and space scales

While exact numbers produced from this effort will only be in terms of a model simulation, trends that show up within the model output should be representative of those found in the real world.

CHAPTER 2 : METHODS

Study Domain

The study domain was chosen to be a square area roughly centered over the UCRB covering an area of approximately 180,000 km² (Figure 2.1) and ranges in elevation from 1115 m to 4384 m. The northern and southern boundaries of the domain are defined by the Colorado state line at approximately 41.0° and 37.0° latitude, the eastern edge by the continental divide of Colorado and the western edge by the Wasatch mountain range in Utah. This domain was chosen by striking a balance between maximum areal coverage and computational resources required to carry out simulations. It encompasses the largest possible area of the UCRB, including most of the high elevation snow accumulation zones while at the same time avoiding areas that lie outside of the UCRB watershed. It is important to note that this domain excludes the Green River portion of the greater UCRB watershed, and results should not be considered representative of the entire UCRB drainage area.

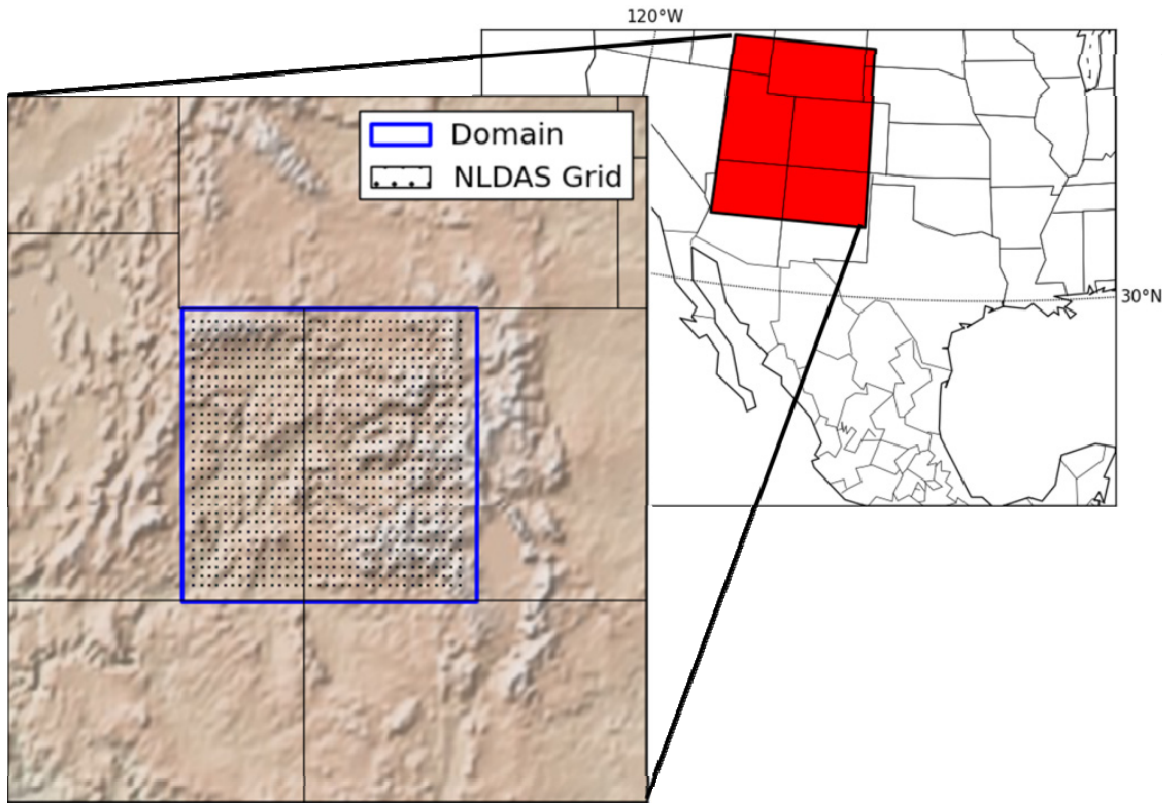


Figure 2.1: Location of study domain and NLDAS grid-points

Land cover, land use and vegetation vary drastically within the study domain, ranging from arid high desert environments of scrubland and short conifer forests in valley locations to dense stands of spruce and pine evergreens in the subalpine forests of the numerous mountain ranges (Figure 2.2). Timberline occurs at approximately 3400 m above sea level, and areas above this generally consist of tundra grasses and small shrubs interspersed among regions of exposed rock.

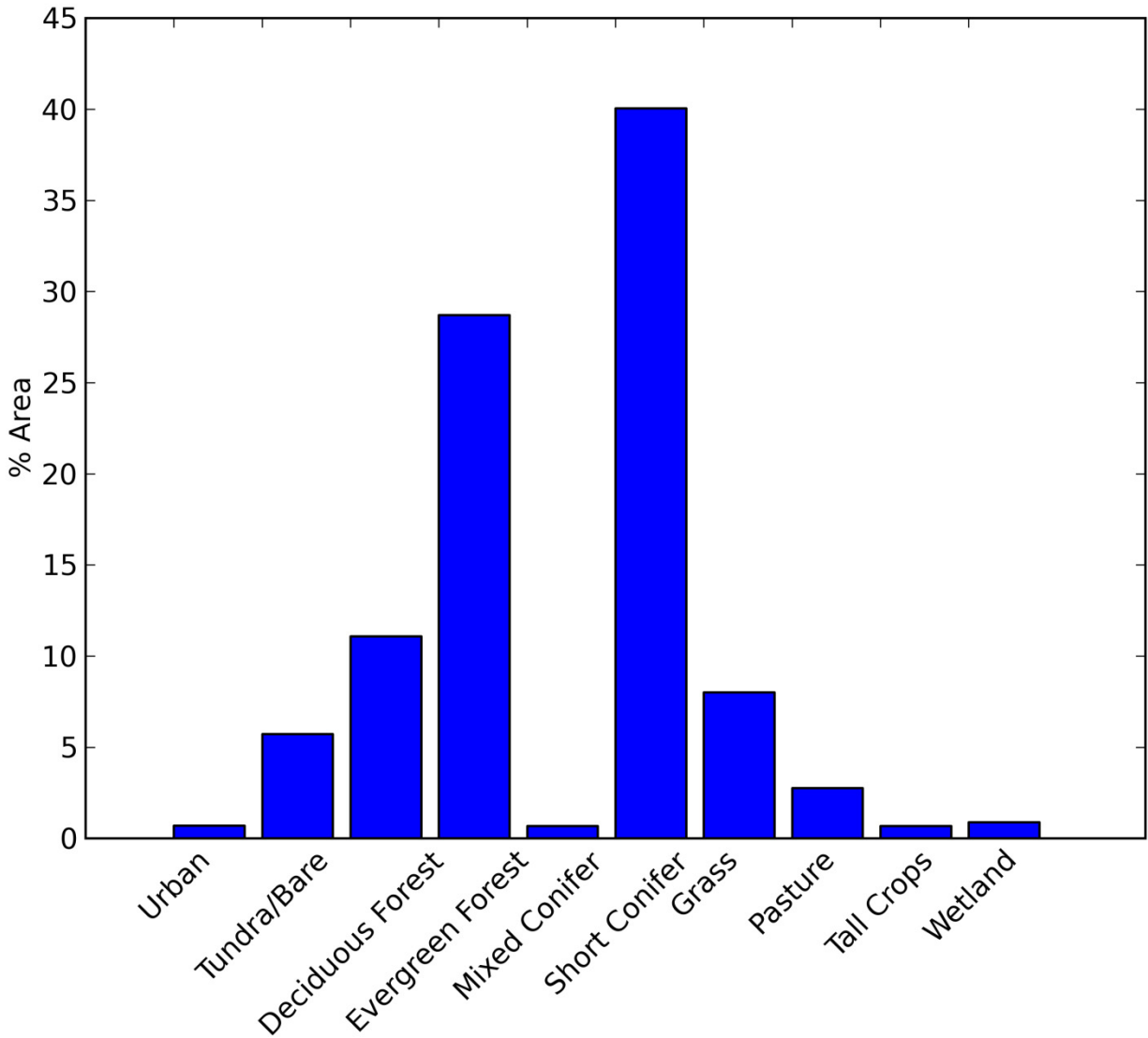


Figure 2.2: Land use types in the study domain derived from the 2006 National Land Cover Database (Fry et al., 2011)

Wintertime meteorological conditions are characterized by sub-freezing temperatures and predominantly westerly flow aloft. Precipitation during the winter is brought almost exclusively by frequent winter storms originating from the Pacific which are enhanced by orographic lifting from the high topography of the continental divide and other mountain ranges. The accumulation season generally begins during early October and lasts through mid-April (depending on elevation and latitude) when peak Snow Water Equivalent (SWE) is reached

(Figure 2.3). The majority of the basin becomes snow free by mid-June on average, with the exception of shaded north slopes and isolated perennial snow fields in high alpine regions. Summertime precipitation is mostly convective in nature, but may fall as snow in the highest elevation regions well into the summer.

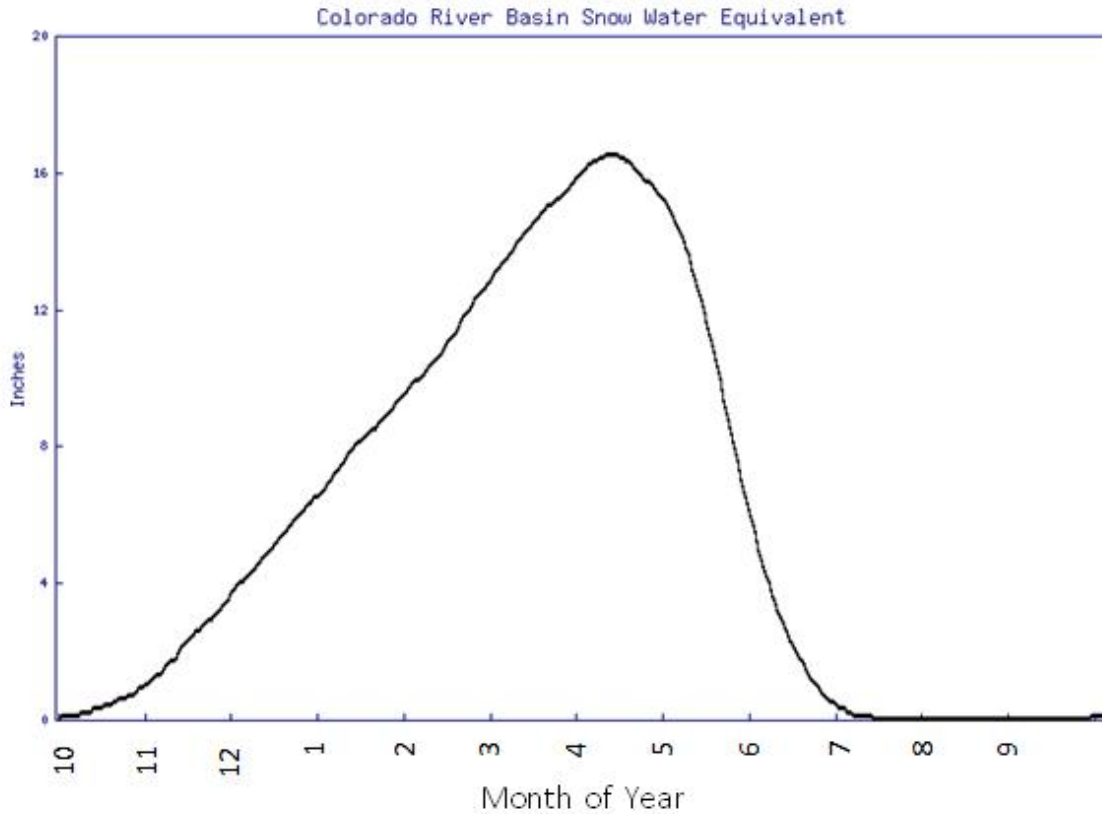


Figure 2.3: 30 year average (1979-2009) SWE accumulation for SNOTEL stations located in the UCRB

Model Description

SnowModel is a spatially-distributed, physically-based snow evolution model driven by input forcing fields of temperature, relative humidity, wind magnitude and direction, and precipitation (Liston et al., 2006). Snow evolution can be simulated on a range of time-steps ranging from sub-hourly to daily and on grid scales from 1 m to 1 km, and is carried out through the use of four primary sub-models. The first of these is the MicroMet sub-model, which

interpolates large scale or station data to the fine scale model grid. The EnBal sub-model is then responsible for calculating the surface energy balance based off of the incoming long and short wave radiation, meteorological conditions and precipitation calculated in the MicroMet sub-model.

These energy fluxes are then combined with additional MicroMet forcing to simulate the evolution of the snow mass in the SnowPack sub-model. Finally, a three dimensional snow transport model called SnowTran3D calculates latent energy fluxes and snow redistribution resulting from model simulated blowing snow. SnowModel also includes SnowAssim, an additional sub-model designed to account for inconsistencies between modeled and observed SWE values. Real world snow observations at specific locations are used to create a correction factor between an initial model run, and then applied backwards in time to nudge the modeled SWE values toward observations at the expense of energy and mass balance.

SnowModel was chosen because of its ability to simulate blowing snow sublimation, thorough documentation and computational efficiency. While many other snow evolution models exist, most lack the combination of previously mentioned attributes which make it feasible to carry out a study of this magnitude using the limited resources available.

Data Description

Due to the extensive area covered by the UCRB, forcing data for the snow evolution model was taken from a gridded reanalysis product rather than individual station data. The sheer volume of processing that would have been required to quality control the hundreds of individual stations inside the basin would have been far beyond the reasonable scope of this project. Rather than attempting to compile and quality control data from point measurements, it was decided that

gridded meteorological data from numerical forecast model re-analysis provided the best balance between ease of access, spatial coverage and continuous record.

Among the most difficult tasks of the study is obtaining the most accurate and fine-scale analysis data to drive the surface snow model. Until recently atmospheric analysis tended to be coarse in resolution (20-40 km) compared to the relatively fine scale at which land surface characteristics may vary, however there has been significant advances in the production of high resolution atmospheric analyses specifically intended for use in land surface modeling. Among the options was an analysis derived forcing dataset from the North American Land Data Assimilation System, which provides surface forcing to run a number of operational products such as the NOAH and VIC land surface models (Mitchell et al., 2004). Favorable validation of the NLDAS data compared to other high resolution atmospheric analysis (Cosgrove et al., 2003), combined with the ease of access granted by NLDAS, led to this data set being chosen as the primary source of surface meteorological data for the study.

The North American Land Data Assimilation System (NLDAS) consists of a series of uncoupled models forced with observations and output from numerical prediction models (Cosgrove et al., 2003, Mitchell et al., 2004). Forcing data for NLDAS is generated both retrospectively and in near real-time at the National Centers for Environmental Prediction using a variety of data sources, and consists of a retrospective archive (1979-2011) and a daily updated archive. Forcing for the non-precipitation fields are derived from the analysis fields of the North American Regional Reanalysis (NARR; Mesinger et al., 2006) that are downscaled from 32 km to the 1/8th degree (~ 14 km) NLDAS grid (Figure 2.1) and then temporally disaggregated to hourly time steps.

The precipitation field is generated through a combination of point measurements from gauge observations and radar based precipitation estimates. CPC daily gauge data adjusted with PRISM climatology provides the main source of the NLDAS precipitation forcing. These data are then temporally disaggregated to an hourly time step using a combination of NWS Stage II hourly precipitation analysis and WSR-88D radar estimates (Cosgrove et al., 2003).

Elevation data were taken from the National Elevation Dataset (Gesch et al., 2009) and land cover data were taken from the 2006 National Land Cover Dataset (NLCD) (Fry et al., 2011). These data were then merged and interpolated to a 250 meter grid resolution using a GIS software package. In the case of the NLCD land cover data, a re-classification between the NLCD land cover types and the land cover types in SnowModel was required. Land cover type re-classification values are detailed in Table B-1, and are consistent with the land cover descriptions of the NLCD and SnowModel cover types including the effective Leaf Area Index (LAI) of forest land cover types found in SnowModel.

Model Configurations

While it would be possible to force SnowModel with retrospective NLDAS forcing data back to 1979, computational limitations restricted the study period to a length of 10 years. For this study the most recent 10 years of hourly forcing data from October 1, 2001 through September 30, 2011 were used. The simulation was carried out for the entire water year (WY) to avoid choosing an arbitrary end to the snow season, considering the wide range of snow free dates within the diverse environments found in the study domain. The model was then run annually for these years at resolution of 250 m and hourly time-steps. A total of 69 SNOTEL measurement locations with at least 10 years of record were chosen for validation and comparison of model output (Figure 2.3). Seasonal cycles of temperature, RH, wind and

precipitation from the NLDAS grid points nearest to these 69 SNOTEL locations averaged over the 10 years of simulations are shown in Figure 2.5.

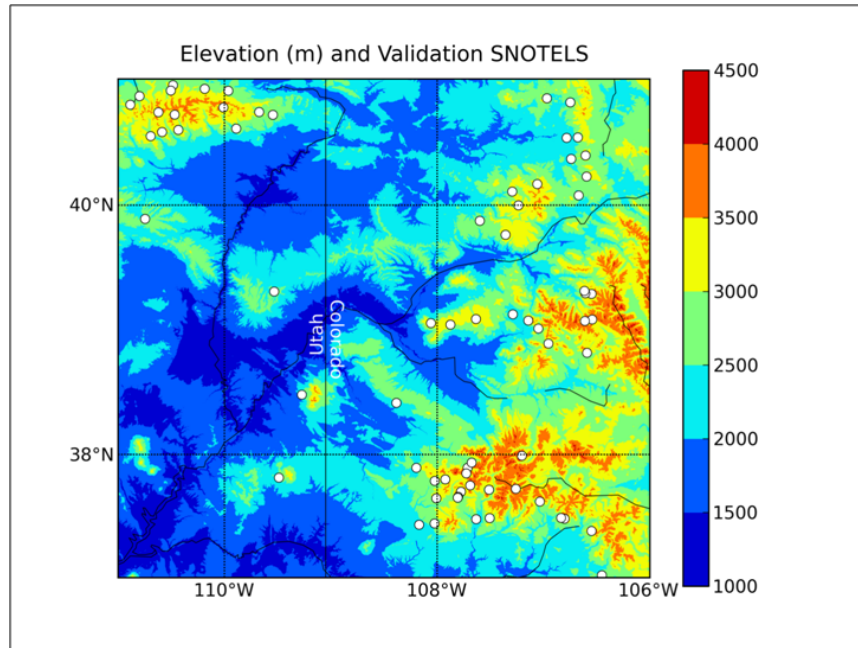


Figure 2.4: Location of SNOTEL sites used for validation and comparison of model results

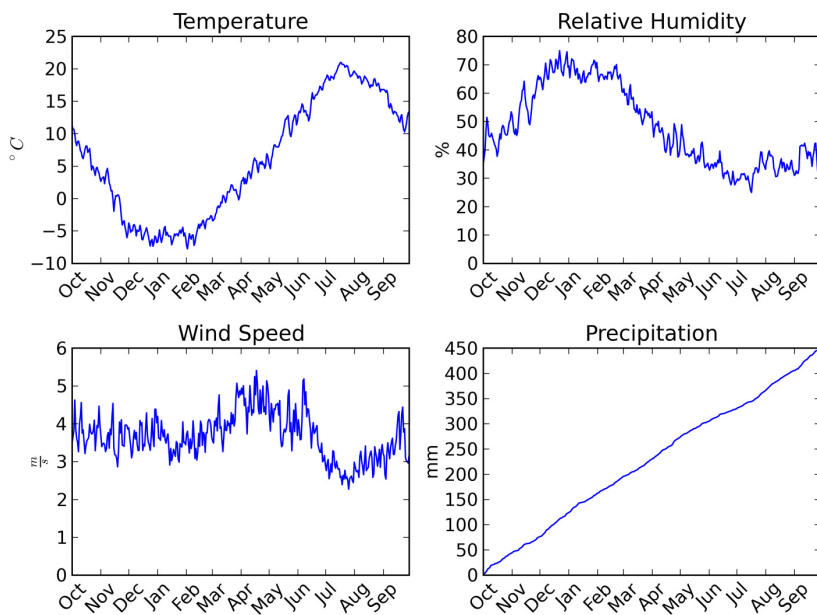


Figure 2.5: 10 year average seasonal cycles of temperature, relative humidity, wind speed and accumulated precipitation over the water year for NLDAS grid points nearest 69 SNOTEL locations

Due to the large volume of data, output data for primary diagnostic fields was only saved at the end of each model day rather than at hourly intervals, and each year of output was immediately archived on a separate data server following completion resulting in an additional 10 hours of transfer time across the network. The external data server contained 2 Tb of storage space with RAID 1 redundancy, and was capable of storing approximately 10 years of daily output from the four SnowModel sub-models.

The program was run serially on a server using a 3.0 GHz Intel processor and 16 Gb of RAM, taking roughly 50 hours of wall time to complete each year of simulation. Simulations for WY 2010-2011 and the LAI sensitivity run were completed using a somewhat less powerful server, and thus resulted in run times of around 80 hours wall time. All simulations were memory intensive, consuming almost 6 Gb of RAM and nearly 200 Gb of output for each year.

Data Analysis

Analysis of the dataset was carried out using the Python programming language, a widely used open source programming language with a wide range of extensible libraries. The Numpy and Scipy extension libraries were used during analysis, and plots were made using the Matplotlib extension.

CHAPTER 3 : RESULTS

Model Results

A negligible amount of accumulated water balance error was recorded over the 10 years simulated. Domain total simulated sublimation by type over the model domain is shown in Figure 3.1. The annual sublimation for all types averaged 1.16×10^7 acre-feet of water over the ten years of simulation. The overall magnitude of total sublimation varied by 68% or between the maximum of 1.37×10^7 acre feet in WY 2005 and a minimum of 0.95×10^7 acre feet in WY 2002. The majority of the sublimation estimated by the model resulted from canopy loss, with sublimation from blowing snow only contributing a small amount to the overall amount of sublimation.

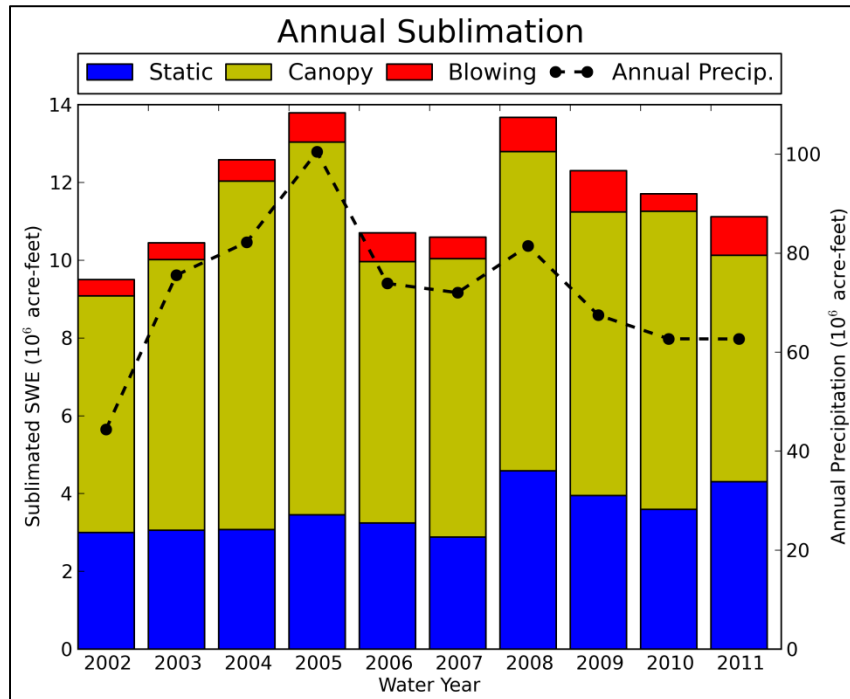


Figure 3.1: Annual Domain total sublimation by type from October 1, 2001 through September 30, 2011

Annual domain total sublimation for each of the components was then weighted by the total area over which that type of sublimation occurred during that year. The result of this analysis shows the relative contribution of each component on an area basis (Figure 3.2). Here it can be seen that the efficiency of blowing snow sublimation rivals that of canopy sublimation, and that static surface sublimation is only about half as efficient at removing water from the snowpack as canopy or blowing snow. In addition, the relative efficiency of each component varies greatly from year to year, with canopy sublimation being more efficient in the first half of the simulations and blowing snow sublimation dominating during the second half.

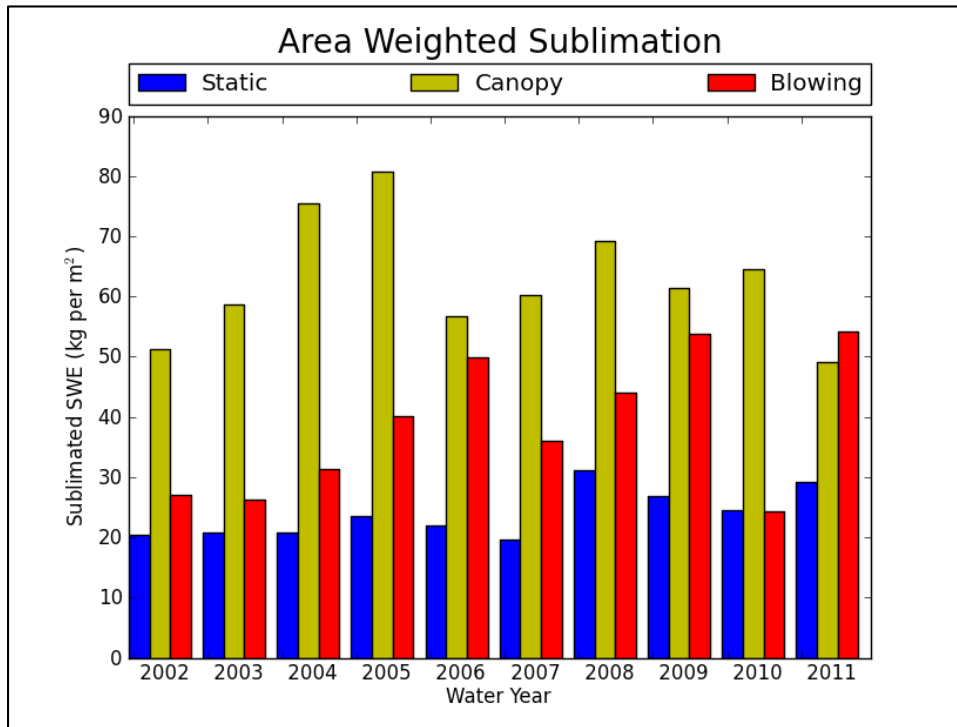


Figure 3.2: Domain total sublimation normalized by area

Daily sublimation values from select sites show that higher rates of sublimation tend to occur during periodic episodes lasting from 2 to 5 days. Spectral analysis of daily sublimation amounts confirms this, with statistically significant peaks at the 5 and 3 day cycles. Outside of these periods of enhanced sublimation, snowpack water loss from all sublimation components

generally remains less than 0.5 mm/day and lasts for several days. The 10 year average annual sublimation from these sites shows that sublimation is maximized from December through May, slowly increasing during the fall accumulation season and quickly ending during melt (Figure 3.3).

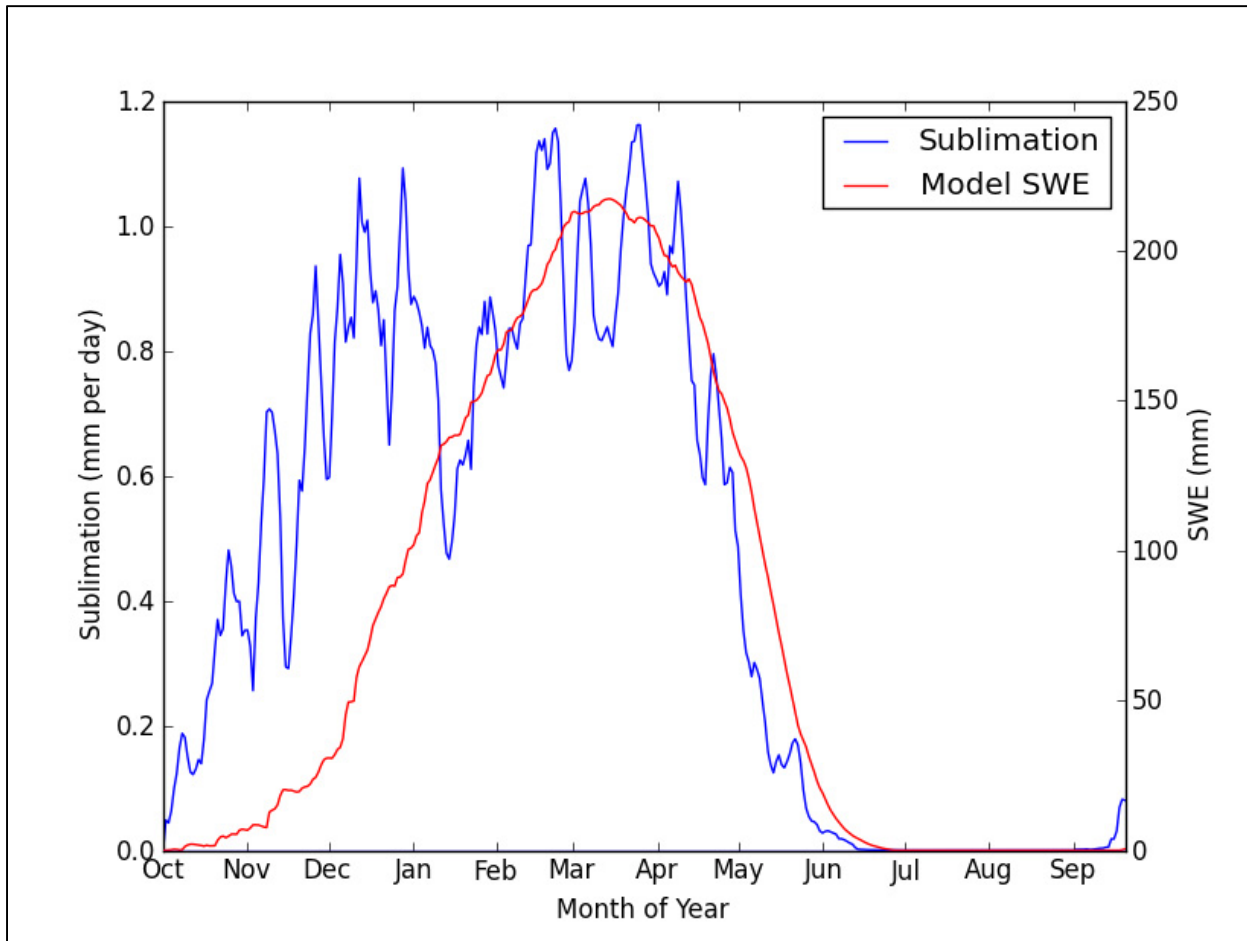


Figure 3.3: 10 Year simulated average daily sublimation smoothed with a 5-day running mean and 10 year average simulated SWE at 69 select SNOTEL sites

The spatial distribution of sublimation throughout the domain is summarized in Figure 3.4, and the by each component in Appendix A. Average annual simulated total sublimation shows a distinct elevation-gradient, maximizing on the windward slopes of alpine regions in central and southern Colorado and minimizing in the drier valley locations. The magnitude of

annual average sublimation ranges from 1-10 mm in the sheltered valleys, to isolated amounts exceeding 500 mm on preferred upwind aspects of high alpine terrain.

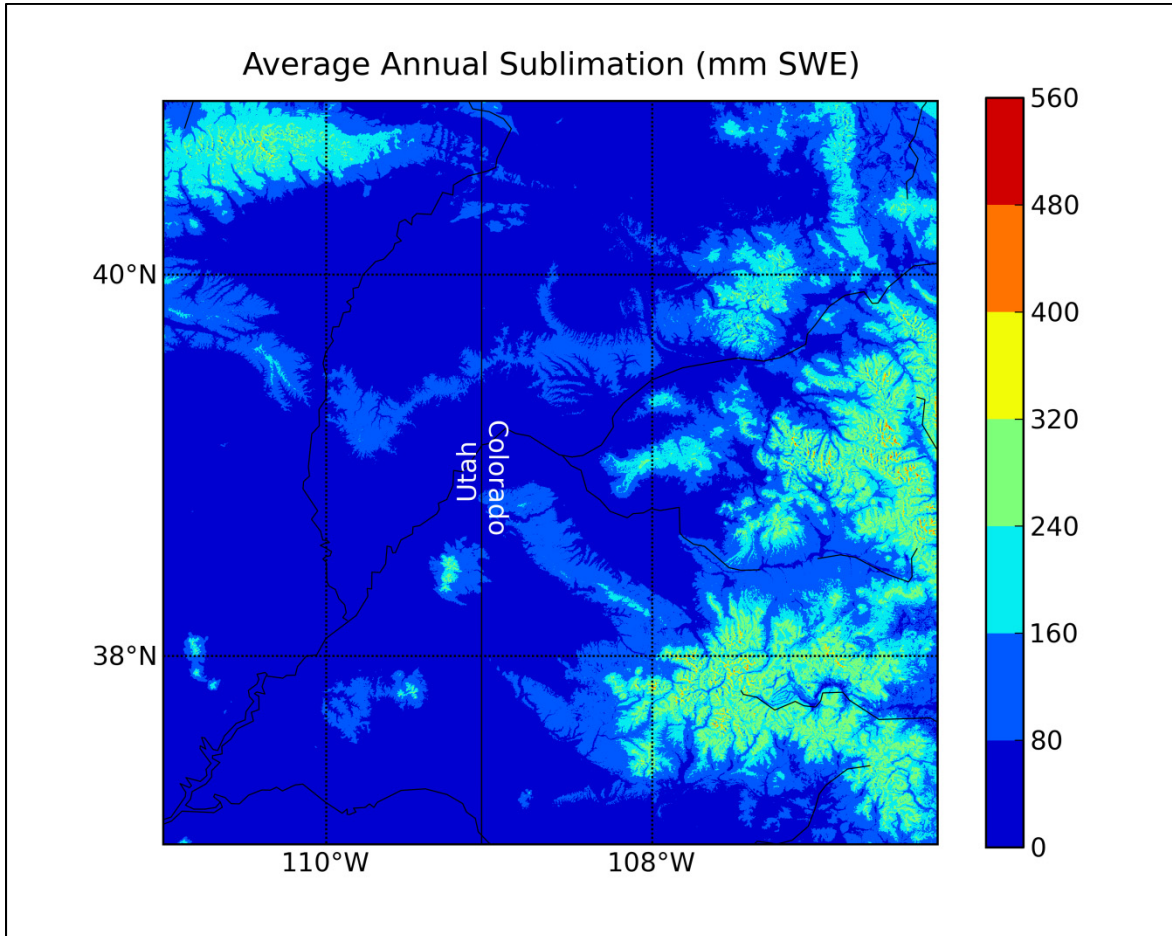


Figure 3.4: Average annual sublimation simulated from October 1, 2001 through September 30, 2011

Daily rates of sublimation were also computed over the entire domain using the difference in total sublimation at the end of each model day (Figure 3.5). Annual averages were computed by only considering days when sublimation occurred at a given grid cell. The spatial distribution of sublimation rate closely follows the distribution of total sublimation, with the highest rates located on the alpine ridgelines.

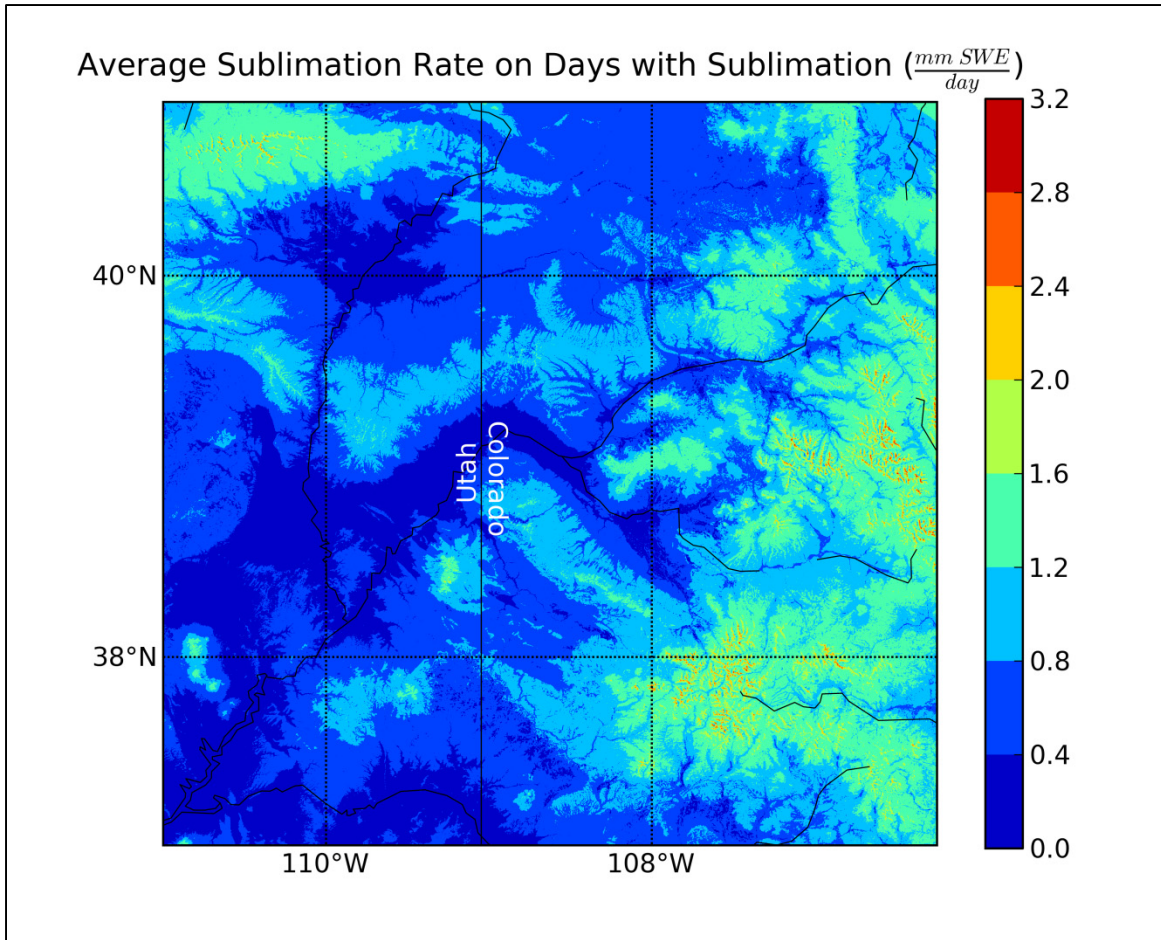


Figure 3.5: Average sublimation rate on days when sublimation occurred from October 1, 2001 through September 30, 2011

A histogram of sublimated water volume is given in Figure 3.6, and shows that the greatest estimates of sublimation come from lower to middle elevations in the 1300-3500 m range. The distribution of elevation throughout the domain (Figure 3.7) shows a similar pattern to the total sublimation volume with a peak around 2000 m.

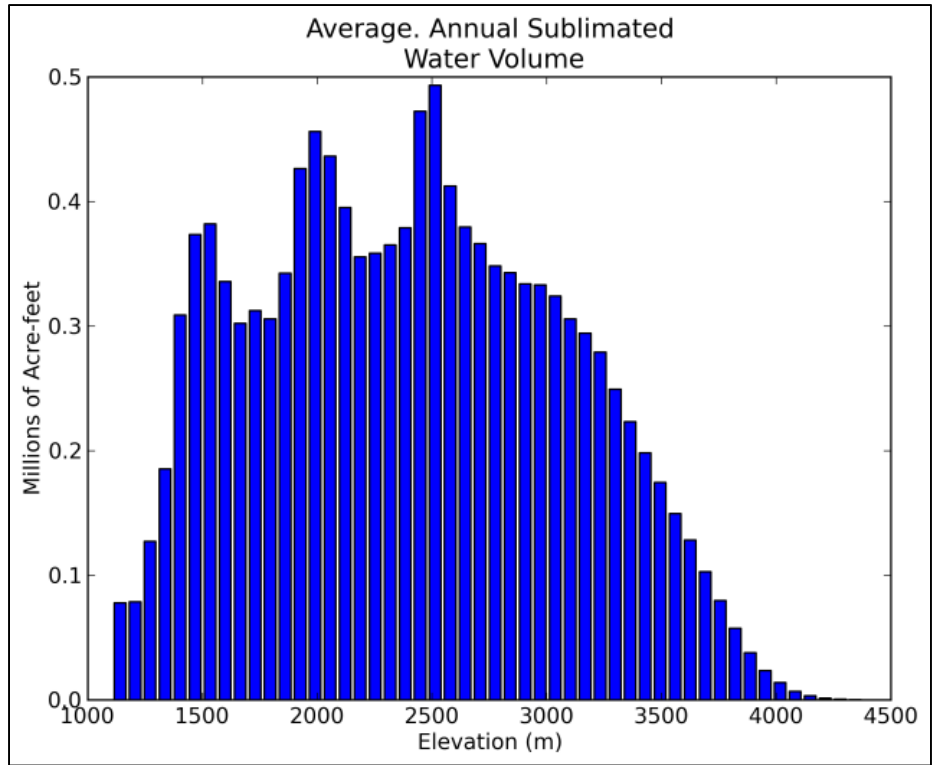


Figure 3.6: 10 year average annual sublimation volume binned by elevation

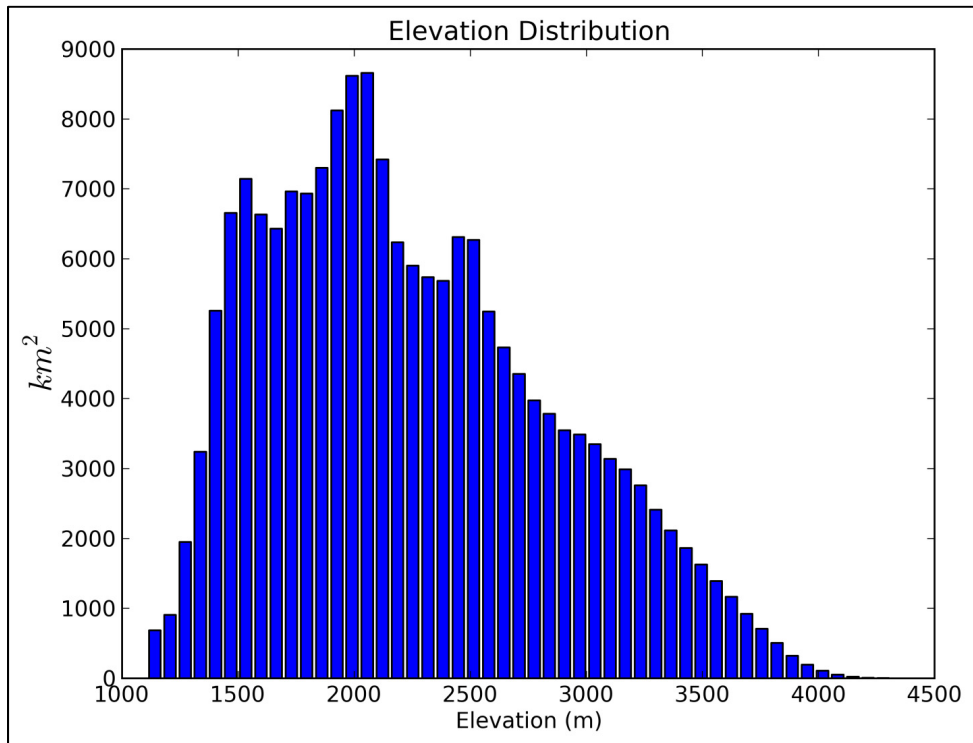


Figure 3.7: Area of study domain binned by elevation

Figure 3.8 shows the same values as in Figure 3.6 normalized by the number of grid cells in each bin to provide sublimation per unit area. Here sublimation is seen to decrease to a minimum at the 1700 m level, then, gradually increases until the 3500 m level. Sublimation above the 3500 m level increases drastically with increasing elevation to a maximum of over 250 mm m^{-2} per year, largely due to the addition of blowing snow sublimation.

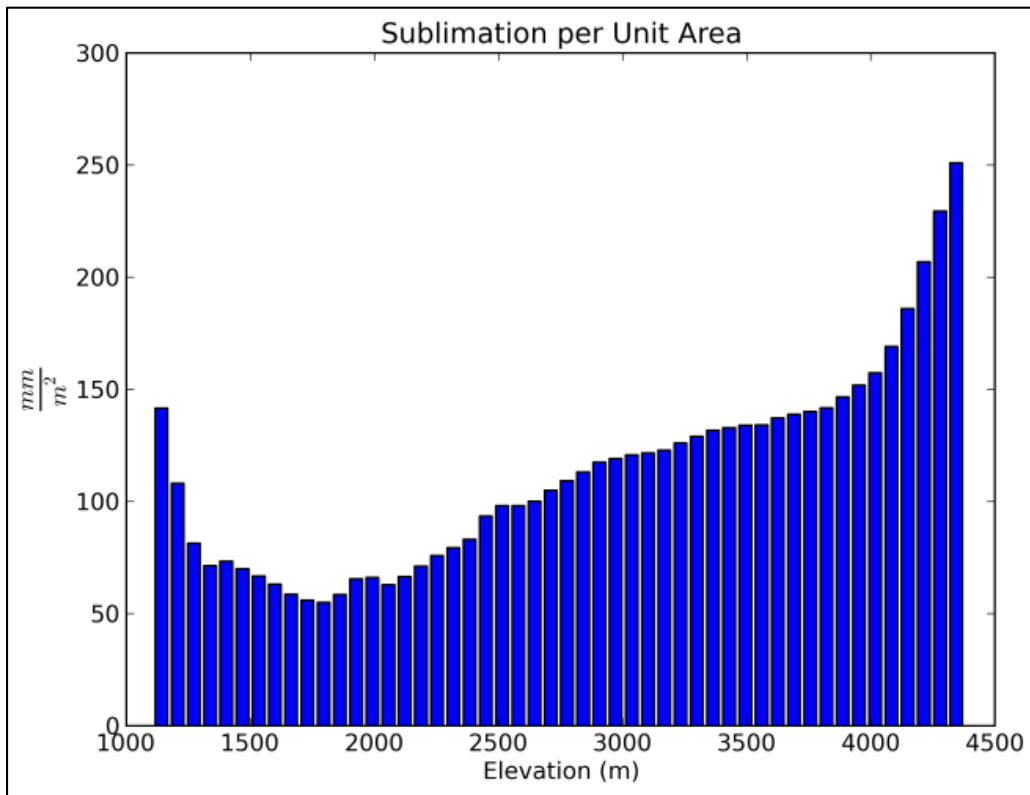


Figure 3.8: 10 year average annual sublimation per unit area binned by elevation

Sublimated precipitation fraction is shown in Figure 3.9, and ranges from 0-4% in the low valleys to 20-30% in the high mountains, with isolated areas exceeding 30% of annual precipitation. These areas of extreme sublimation loss coincide with the same areas which experience extreme daily sublimation rates.

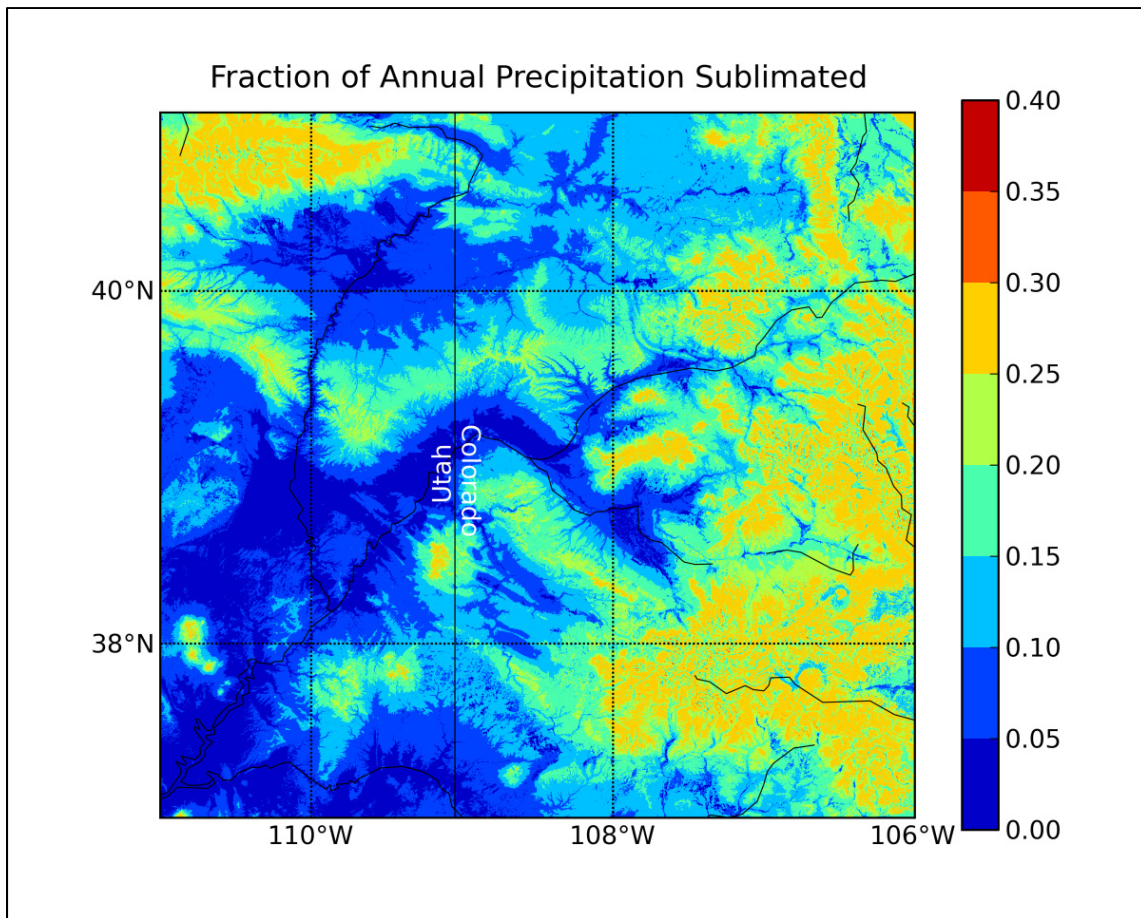


Figure 3.9: 10 year average of annual fraction of sublimated precipitation

Validation/Comparison with Precipitation Observations

Validation of the model results was carried out for both precipitation and accumulated SWE fields using observations collected by the Snowpack Telemetry (SNOTEL) network. It is important to note that the SNOTEL observations used in the validation were also incorporated into the precipitation forcing from the NLDAS data; however, these observations were considered the best option for comparing model output given the relative lack of consistent, long term data in the snow accumulation zones. Furthermore, the NLDAS analysis does not weight single-point data heavily. Stations were required to have at least a 10 year data record and contain no more than 5% of missing values throughout the record. A total of 69 SNOTEL

stations meeting this criterion were identified within the model domain, and the corresponding model grid cells then manually located. Daily measurement values of precipitation and SWE were used, and any missing values within the observation record were discarded. Analyses were then carried out for each individual year of simulation from October 1, 2001 through September 30, 2011 (Appendix C).

Simple least squares correlation analysis show reasonable agreement between model derived precipitation and observed precipitation, with 10 year regression coefficient of 0.65 and a correlation coefficient of 0.76 (Figure 3.10). Comparison between model-derived SWE values and SNOTEL observations showed a poorer relationship than the precipitation fields, with a 10 year regression coefficient of 0.38 and a correlation coefficient of 0.63 (Figure 3.11). Sample size for the precipitation validation was 251118, and for the SWE validation was 251100, and spanned the entire water year. Validation also appeared to be site specific, with some model grid cells consistently over or under estimating both precipitation and SWE values.

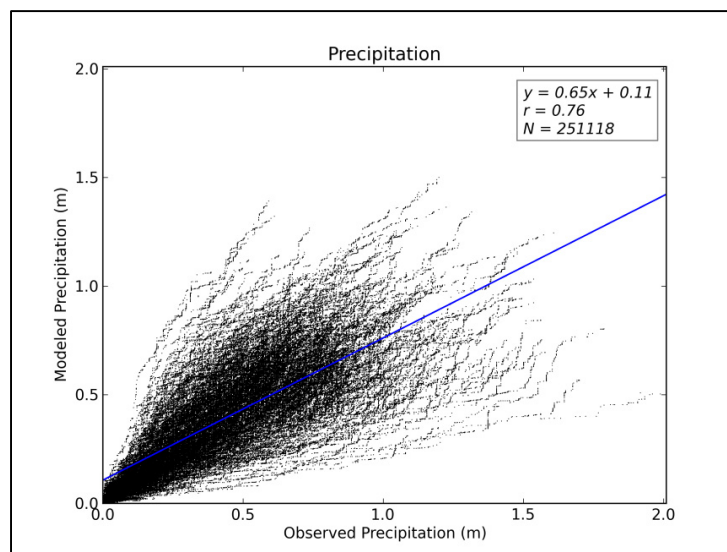


Figure 3.10: Comparison of observed precipitation from 69 SNOTEL sites to model simulated precipitation

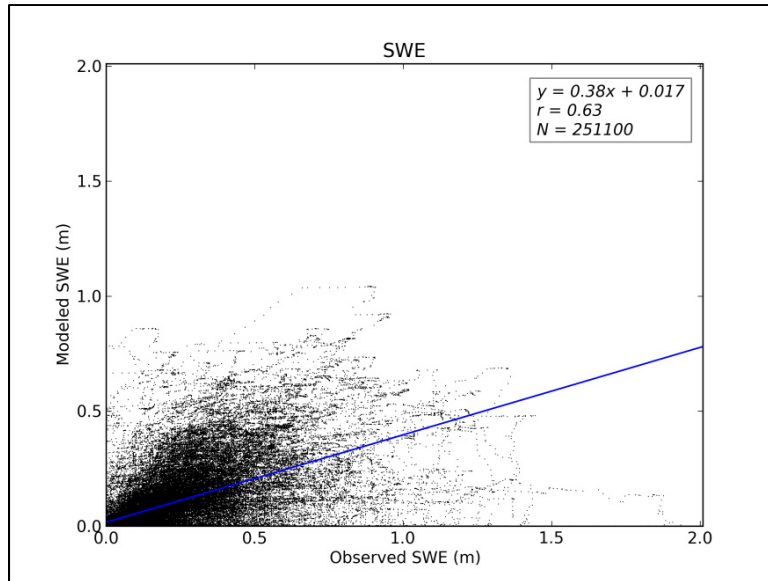


Figure 3.11: Comparison of observed SWE values at 69 SNOTEL sites to model simulated SWE values

Sensitivity Analysis

Canopy Sensitivity

An additional simulation was carried out to test for the sensitivity of SnowModel's canopy sublimation to the LAI of the model. LAI values for the individual land types were altered following estimates made on Lodgepole Pine stands (*Pinus contorta*) impacted by the Western Mountain Pine Beetle in western North America (Pugh et al., 2012). LAI for the conifer land type was reduced by 30% and by 10% for the mixed conifer/deciduous land type. LAI was held constant for the short conifer land class because it consists of tree species that have been significantly impacted by the mountain pine beetle. A one-year simulation for WY 2004-2005 was then run using the altered values of LAI and output saved at the end of each model day (Figure 3.12).

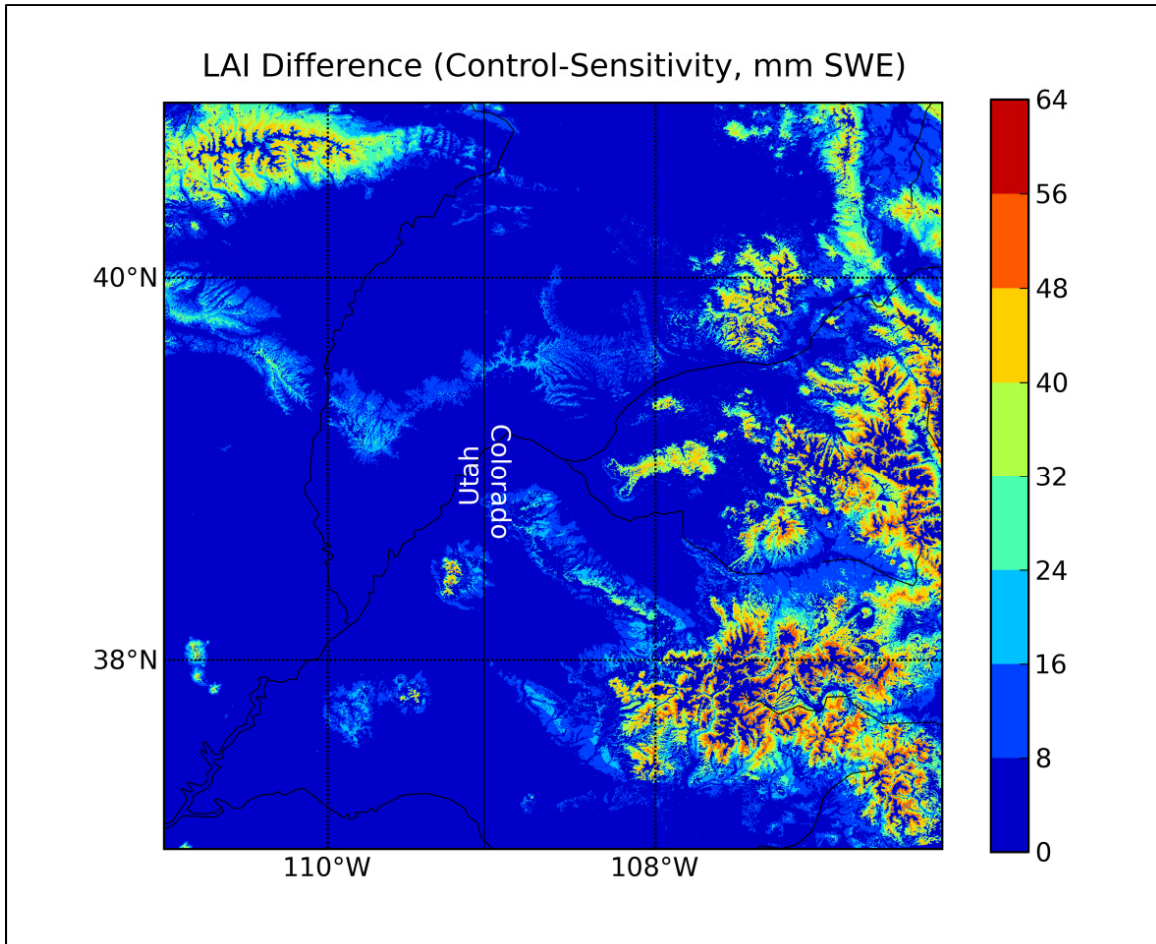


Figure 3.12: Difference in simulated canopy sublimation between the control and a 30% reduction in LAI sensitivity run for WY 2004-2005

Results from this reveal a 10% (1.01×10^6 acre-feet) decrease in annual canopy sublimation over the domain, with a corresponding 7% (0.26×10^6 acre-feet) increase in static surface sublimation compared to the control run. Changes in the amount of blowing snow sublimation were negligible ($\ll 1\%$). The overall change in total sublimation for the sensitivity run is 5% (0.75×10^6 acre-feet) less than in the control run. Reduction in LAI also resulted in a 2% (0.10×10^6 acre-feet) increase in canopy unloading and a decrease of 15% in average domain canopy storage. Additional runs were made for the same water year with a 15% and 60%

reduction in LAI to test the models sensitivity to various LAI values, with a near linear trend in resulting sublimation changes (Figure 3.13).

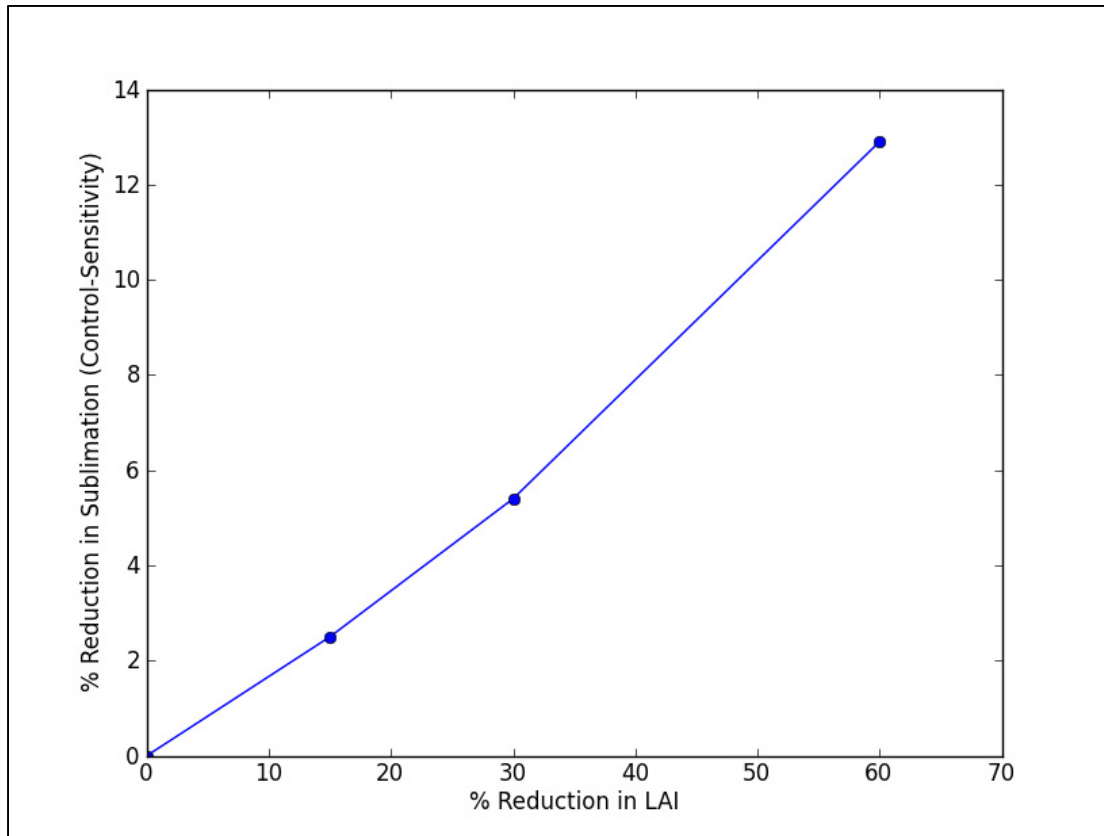


Figure 3.13: Percent reduction in LAI vs. percent reduction in total sublimation

CHAPTER 4 : DISCUSSION

Static Sublimation

The static sublimation component accounts for the smallest overall magnitude of mass flux even though it occurs over a larger land area than either blowing or canopy sublimation. Compared to blowing snow and canopy sublimation, static surface sublimation is a relatively inefficient means of sublimation due to the limited area of snow surface exposed to the atmosphere. Static sublimation is further reduced by the dense vegetation stands located over much of the lower elevation accumulation zones; however, above tree line the effects of increased ventilation are apparent, with 10 year average annual sublimation amounts exceeding 100 mm.

Static sublimation is calculated from the latent heat flux in the EnBal module as (Liston et al., 1995)

$$Q_e = \rho_a L_s D_e \zeta \left(0.622 \frac{e_a - e_s}{P_a} \right) \quad [11]$$

where ρ_a is the air density, L_s is the latent heat of sublimation, ζ is a non-dimensional stability function, P_a is the atmospheric pressure, e_a and e_s are the actual and saturation vapor pressures and D_e is the exchange coefficient. The effect of wind speed on static sublimation can be seen in the exchange coefficient term

$$D_e = \frac{\kappa^2 U_z}{\ln \left(\frac{z}{z_0} \right)^2} \quad [12]$$

where κ is von Karman's constant, z and z_0 are the respective observation and roughness heights and U_z is the wind speed at reference height z . Latent heat transport, and therefore sublimation, is directly proportional to wind speed at the snow surface. From this it can be seen that sublimation will occur at almost all times provided that at least some vapor pressure deficit exists and there is a non-zero wind speed.

Blowing Snow Sublimation

One of the reasons SnowModel was chosen for use in this study was its ability to explicitly simulate blowing snow processes, and the results from the SnowTran sub-model confirm the idea that blowing snow sublimation plays a significant role in the alpine snow water balance. The extreme conditions of sustained high velocity winds, intense solar radiation and large potential vapor pressure deficits found in high elevation environments leads to very efficient mass transfer from solid to vapor phase.

Sublimation from blowing snow in SnowModel is represented by

$$Q_v(x^*) = \psi_s \varphi_s z_s + \int_0^{z_t} \psi(x^*, z) \varphi(x^*, z) dz$$

where the sub-scripts s and t represent saltation and turbulent suspension respectively, x^* (m) is the wind flow relative horizontal coordinate, z (m) is the height coordinate, ψ (s^{-1}) is the sublimation-loss-rate coefficient, φ ($kg\ m^{-3}$) is the suspended snow mass concentration and z_t (m) is the top of the saltation/turbulent suspended snow layer (Liston et al., 1998). The influence of ventilation on sublimation can be seen in the sublimation coefficient term as (Pomeroy et al., 1991)

$$\psi = \frac{1}{m} \frac{dm}{dt} = \frac{1}{m} \frac{2\pi r \left(\frac{RH}{100} - 1 \right) - \frac{S_p}{\lambda_t T_a Nu} \left[\frac{h_s M}{R T_a} - 1 \right]}{\frac{h_s}{\lambda_t T_a Nu} \left[\frac{h_s M}{R T_a} - 1 \right] + \frac{1}{D \rho_v Sh}} \quad [3]$$

where Nu and Sh are the Nusselt and Sherwood numbers respectively. Letting $Nu \cong Sh$ (Thorpe et al., 1966) and using $Nu = 1.79 + 0.606(Re)^{0.5} = 1.79 + 0.606 \left(\frac{2rU_w}{\nu} \right)^{0.5}$ (Schmidt et al., 1991) yields

$$\begin{aligned} \psi &= \frac{1}{m} \frac{2\pi r \left(\frac{RH}{100} - 1 \right) - \frac{S_p}{\lambda_t T_a Nu} \left[\frac{h_s M}{R T_a} - 1 \right]}{\frac{h_s}{\lambda_t T_a Nu} \left[\frac{h_s M}{R T_a} - 1 \right] + \frac{1}{D \rho_v Nu}} \\ &= \frac{1}{m} \frac{2\pi r \left(\frac{RH}{100} - 1 \right) - \frac{S_p}{\lambda_t T_a} \left[\frac{h_s M}{R T_a} - 1 \right]}{\frac{h_s}{\lambda_t T_a} \left[\frac{h_s M}{R T_a} - 1 \right] + \frac{1}{D \rho_v}} Nu \\ &= \frac{1}{m} \frac{2\pi r \left(\frac{RH}{100} - 1 \right) - \frac{S_p}{\lambda_t T_a} \left[\frac{h_s M}{R T_a} - 1 \right]}{\frac{h_s}{\lambda_t T_a} \left[\frac{h_s M}{R T_a} - 1 \right] + \frac{1}{D \rho_v}} \left(1.79 + 0.606 \left(\frac{2rU_w}{\nu} \right)^{0.5} \right) \quad [4] \end{aligned}$$

This form of the sublimation coefficient shows how the rate of sublimation is proportional to the square root of the wind velocity. The influence of wind illustrates the effect that highly ventilated environments, like those found at high elevations, have on the rate of sublimation within the model where the sublimation coefficient increases rapidly with greater wind speeds.

Simulated blowing snow sublimation amounts agree with previous studies using SnowModel, where sublimation on exposed ridgelines often exceeds 500 mm annually. Because SnowTran assumes that the transport flux of blowing snow is in equilibrium with the wind field

it neglects the effects of suspended snow plumes resulting from flow separation along steep ridges, a phenomenon often observed during clear, windy days on alpine peaks (Liston et al., 2007). The suspension of large plumes of snow out of the near-surface boundary layer is a potentially significant sublimation loss process not represented in the model, and the actual amount of sublimation occurring in the alpine environment could reasonably be higher than reported here.

There also remains the issue of how sublimation, especially from blowing snow, acts to modify the boundary layer through the addition of water vapor and thermodynamic feedbacks. Sublimation acts as a source of moisture and a sink for sensible heat within the turbulent boundary layer, and thus has been argued to modify the temperature and humidity profile as sublimation takes place (Déry et al., 1998). For the case of SnowModel, these feedbacks have been neglected (Liston et al., 1998) and represents another source of uncertainty in estimates of sublimation. While these feedback effects would be useful for making the model more representative of the real world, they are also computationally expensive and would result in limitations elsewhere in the model.

Canopy Sublimation

The relatively high contribution of the canopy component to domain total sublimation attests to the efficiency of mass transfer of intercepted snow within the model, and is of particular interest given the widespread pine forests characteristic of the snow accumulation zones in the UCRB.

Results from the canopy component of sublimation show an average loss of $5.05 \times 10^7 \frac{kg}{km^2}$, which is in-line with conservative estimates that show canopy sublimation of $4.47 \times$

$10^7 \frac{kg}{km^2}$ for a forested watershed in western Canada (Schmidt et al., 1992). These results show that the model simulated sublimation that were comparable to estimates made from actual observations, and reinforces the idea that sublimation returns a large portion of snowpack water to the atmosphere.

Sublimation of snow stored in the canopy is calculated as

$$Q_{CS} = C_e I \psi(x^*, z) dt \quad [5]$$

where $\psi(x^*, z)$ is the sublimation coefficient as in [3], C_e is non-dimensional canopy exposure coefficient that accounts for exposed snow surface on the intercepted snow and I is the intercepted canopy load. In this case the sublimation is enhanced by both the higher wind speeds found in the canopy and the increase in surface area represented by C_e .

Land surface characteristics, particularly those of forests, have the ability to vary on short timescales, with extreme events such as fires resulting in changes to a large area of the surface environment in only a matter of days to weeks. In the case of the UCRB, impacts from various species of bark beetle (*Coleoptera: Scolytidae*) have led to widespread tree mortality and subsequent reduction in the canopy density which may not be represented in either the land use data or in the model parameterizations.

Changing the value of the LAI for forest land cover types will directly impact the calculated sub-canopy wind speed, $U_{subcanopy}$, which is given by

$$U_{subcanopy} = e^{\left(-(0.9 LAI^*) \frac{(1 - (0.6 H_{veg}))}{H_{veg}} \right)} U_{grid} \quad [6]$$

where LAI^* is the effective LAI of the forest land cover type, H_{veg} is the vegetation snow holding capacity height and U_{grid} is the interpolated wind speed. Here it can be seen that reducing the LAI will lead to an increase in the sub-canopy wind speed, and thus increase the mass transfer from solid to vapor phase in the forest environment via equations [1] for static surface sublimation and [5] for canopy sublimation. Altering the LAI will also modify the surface radiation balance by allowing more shortwave to penetrate to the surface and reduce long-wave attenuation by the canopy. Unfortunately the coarse temporal resolution of the daily output produced by the model limited the ability to determine to what degree each of these factors influenced the simulated sublimation, as they vary on hourly timescales.

The sensitivity run of reduced LAI illustrated that changes to the forest canopy density led to corresponding changes in the amount of canopy and static surface sublimation, with a net decrease in domain total sublimation of 5%. Doubling the LAI reduction leads to an even greater reduction in sublimation, decreasing the canopy component by almost 12% from the control run (Figure 3.13). Even though this number is only a small fraction of the overall sublimation budget, it equates to approximately 750,000 acre-feet of water, or an equivalent 5 mm of additional SWE over the entire domain. The impact of this change in the water balance is important because the additional snow not sublimated in the canopy will be added to the sub-canopy snowpack, which is in a relatively low sublimation environment that allows snow to melt rather than sublimate. In terms of the local water balance, retaining this water would result in at least some additional runoff, and could represent a net contribution to the overall water supply in the UCRB. This effect would be tempered by the non-uniform pattern of infestation, as a permanent reduction in LAI is unlikely given re-growth and replacement.

Additional sensitivity runs show that this relationship is approximately linear with LAI reduction, and that simulated canopy sublimation is strongly dependant on the amount of snow intercepted by vegetation. In the case of the UCRB, reductions in LAI from mountain pine beetle mortality are far from homogenous in space and time, and includes tree stands in various stages of mortality and regeneration. Results from this analysis show that the 5% reduction in sublimation calculated following the worst case scenario that assumes 30% LAI reduction given by Pugh et al. is overdone, as not all of the forested areas are likely to be in this stage at the same time. Nevertheless, this illustrates the effect that forest canopy conditions can have on the local water balance regardless of precipitation or meteorological conditions.

Simulating the evolution of snow in the canopy is one of the most difficult tasks due to the highly variable nature of interactions between vegetation and hydrologic processes, a good example being the unloading of canopy intercepted snow. SnowModel uses a melt unloading scheme that assumes a constant unloading rate for above freezing given by

$$L_m = 5.8 \times 10^{-5}(T_a - 273.16)dt \quad [71]$$

where $L_m(kg m^{-2})$ is the unloading rate (assumes $5 kg m^{-2} day^{-1}$), T_a is the air temperature and $dt(s)$ is the time step. Unfortunately this parameterization does not allow for intermittent unloading events due to wind movement. The inability to explicitly simulate wind-induced unloading is desirable because unloaded snow in the low solar insolation, low wind speed and high relative humidity environment of the sub-canopy experiences far less sublimation than would snow within the canopy. Much more could be learned from examining how sublimation from greater sub-canopy wind speeds interacts with increased unloading of the canopy store into the snowpack, especially given the results of reduced LAI on canopy sublimation.

Temporal Variability

Throughout the 10 years of simulations performed, the absolute magnitude of sublimation was found to have a great deal of year to year variability, closely following the domain total precipitation. Larger sublimation amounts for years with greater precipitation is due to the larger snow covered area and longer duration of the snow-pack which allows for more mass flux, consistent with previous findings (Kattleman et al., 1991). Percentage of sublimation loss follows a similar trend. Individual components of sublimation also show a remarkable year to year variability, particularly the blowing and canopy components of sublimation. Despite these inter-component changes, the over-all magnitude of sublimation shows no clear trend across the 10 years of simulations.

In the case of the blowing snow sublimation, WY 2008-2009 and WY 2010-2011 proved to be an anomalously high year, suggesting stronger forcing by the wind field (Figure 3.2). Wind speeds were indeed higher in the NLDAS forcing fields during these years, with WY 2008-2009 having the second highest average wind speed and WY 2010-2011 having the highest wind speed at 69 SNOTEL locations (Figure 4.1). Unfortunately the daily resolution of output data fields does not allow for a detailed examination of the simulated wind field to determine the degree to which it is related to sublimation within the model itself.

The cycling between dominant sublimation components between the years is also of interest. Sublimation efficiency (e.g. the amount of water sublimated per area over which the sublimation type occurs) is dominated by the canopy during the early years, but becomes dominated by blowing snow sublimation later in the period (Figure 3.2). This same trend is seen in the domain total sublimation where canopy sublimation becomes a smaller percentage of total sublimation toward the later years. Analysis of the forcing data at the 69 select SNOTEL sites

reveals that wind speed over this time period did increase from an annual average of 3.6 m/s to 4.0 m/s throughout the 10 years of simulations (Figure 4.1), consistent with a greater contribution to sublimation by the blowing snow component. Although a direct relationship between wind speed and dominant sublimation mode would be intriguing, verification from observations and independent sources is needed to confirm that this hypothesis is valid.

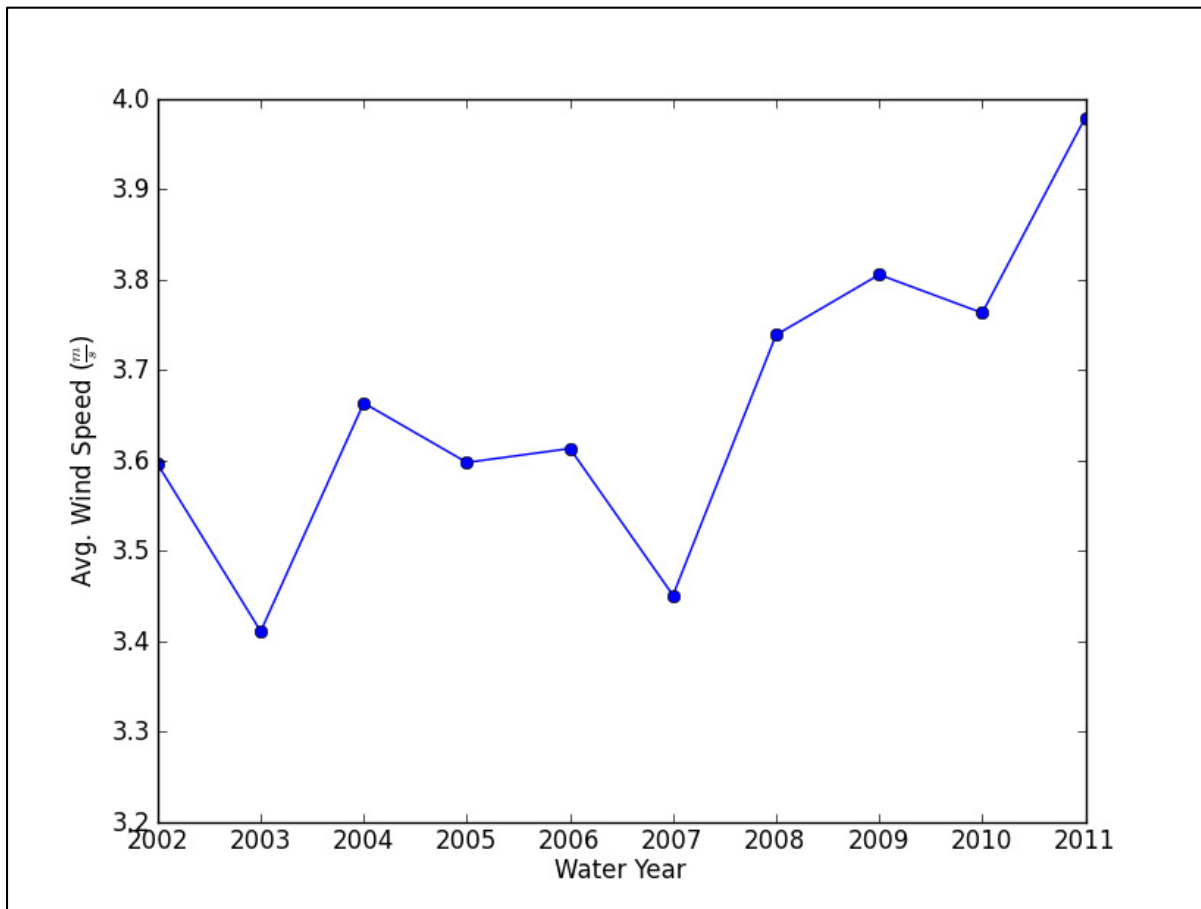


Figure 4.1: Annual average wind speed from the NLDAS grid points nearest the 69 select SNOTEL sites

The annual cycle of sublimation generally follows results from previous studies (Hood et al., 1999) that show the majority of sublimation occurs during the mid-winter snow accumulation season (Figure 3.3). It is during this time period that high wind speeds combine with low moisture content air to maximize mass flux and rapidly deplete the snowpack. The close track of

daily sublimation to the snow accumulation curve illustrates the strong dependence of sublimation on available snow cover.

Sublimation peaks during the late winter and early spring period when wind speeds are greatest and average RH values begin to decline. This is important, because it roughly corresponds to peak SWE accumulation when most water supply forecasts are being made. As a result sublimation loss at this time of year has the potential to lead to overestimation of water stored in the snowpack.

Sublimation also shows interesting temporal variability on sub-annual timescales. Results show that sublimation has a tendency to occur during discrete time periods of enhanced mass flux which are then followed by corresponding periods of little or no sublimation, in line with previous work (Hood et al., 1999). Sublimation events tend to occur in cycles of about 3 to 5 days, and are followed by several days of relatively low sublimation.

These short time scale oscillations are likely driven by synoptic scale variability in the environment associated with passing baroclinic systems that lead to periods of low vapor pressure deficits and weak winds, followed by drying and increased temperatures. The magnitude of sublimation also varies greatly from event to event, with the largest events or 'sublimation storms', removing more than 10 mm of water from the snowpack over a period of a few days. This hypothesis agrees with observations by Hood et al. who note that sublimation events east of the continental divide in Colorado corresponded to down slope Chinook winds known for their dry, warm characteristics. They also point out that even during periods of low sublimation, the cumulative effect of persistent mass transfer results in significant losses of SWE.

Spatial Variability

Results from the model simulations reveal an increase in sublimation across gradients of elevation throughout the domain. Not only do high elevation areas lose the most water from solid phase transition, but they lose it at a greater rate than low elevation areas. This characteristic is best illustrated when considering the annual sublimation bins normalized by the number of grid cells in each bin (Figure 3.8). At altitudes above 3500 m the increasing trend in sublimation becomes almost exponential, and is likely a demarcation of the typical altitude where blowing snow sublimation becomes a more dominant component of the sublimation budget by allowing for more efficient mass transfer.

Analyses of daily sublimation rate reinforces this finding, showing the highest rates of up to 3 mm/day in the high alpine regions. While such mass transfer rates appear to be quite high, they are only a third of the almost 9 mm/day reported by lysimeter measurements made in northern Arizona under clear, windy conditions (Avery, 1992). In fact, such high sublimation rates appear to be typical for mountain ranges found in desert environments, with Schultz and workers reporting rates of 3 to 5 mm/day and results from the White Mountains of California suggesting even greater rates (Beaty, 1975). All of this evidence indicates that the calculated rates of daily sublimation found in this study are well within the bounds of previous research.

A similar pattern is found in the annual sublimated precipitation fraction (Figure 3.9), with the greatest loss of precipitation occurring in the highest elevations and lesser amounts in valley locations. These numbers appear reasonable compared to those found in previous studies that show between 10% and 30% of annual precipitation is returned to the atmosphere via sublimation.

This relationship of increasing sublimation with altitude has profound implications on the role that sublimation plays in the water balance of mountain environments, indicating that the greatest impact from sublimation is felt in areas with the highest concentration of snow pack water. The highly ventilated, low pressure environment of these alpine zones provides adequate driving force to efficiently transition mass from the solid to vapor phase, and also has a large reservoir of water to act upon. These efficient transfer conditions lend credence to the idea, suggested by Schmidt et al., that sublimation acts as a source of atmospheric water vapor (Schmidt et al., 1992) and significantly alter the characteristics of the atmospheric boundary layer.

Despite the relative importance of the alpine zones to sublimation, the sub-alpine forest also lends greatly to the annual sublimation budget. These areas show the largest overall loss of water to sublimation, due in part to the increased ventilation brought about by interception of snow in the elevated tree canopy and a large area over which it occurs (Figure 3.7). Sublimation within these zones is characterized by the availability of snow in the canopy store, unlike the alpine zones where lack of dense vegetation allows for the surface snow to be available for efficient sublimation.

The relationship between wind speed and sublimation is also less clear at these lower elevations, where in the real world high winds may act to unload intercepted snow from the tree branches in addition to aiding in sublimation as discussed in Canopy Sublimation.

Additional Concerns

One of greatest difficulties in conducting high resolution numerical modeling is the sheer volume of data involved. In the case of this study the domain was made up of almost 3 million

grid cells, and while it would have been desirable to retain output of many fields at hourly resolution the space required to do so was considered unfeasible. Doing so would have allowed for a more robust analysis of how each of the relevant fields impacts sublimation within the model, specifically the wind fields, as it is among the most influential factor in determining sublimation.

Another concern that should be addressed is the implementation of radiation and cloud cover in the model. Cloud cover, and thus the resulting radiation budget, are driven by interpolating surface RH to 700 mb using a fixed lapse rate. This method is obviously not appropriate for a number of conditions, for example underneath strong inversions, where high RH near the surface could lead to anomalously cloudy conditions. While this is recognized as a weakness in the model parameterization, past studies have shown that the influence of ventilation is the dominant process (Thorp et al., 1966, Neumann et al., 2008), and errors introduced through misrepresentation of radiation components are not anticipated to lead to significant changes in the results. Regardless, it would be ideal to explicitly prescribe the cloud cover fraction so as to account for changes in the near-snow-surface air temperature, and therefore vapor pressure deficit, brought about by long and short wave radiation fluxes influencing the near-surface temperature profile.

Model Performance

Precipitation Validation

Validation of model grid cells corresponding to the location of SNOTEL observations provided somewhat satisfactory results, with a general underestimation of precipitation by the model. Despite this shortfall on precipitation, the correlation coefficient shows reasonable

agreement between precipitation in the model and in the real world with an r value of 0.76. The model appears to do better on some years than others, with a large spread in regression coefficients between individual years (Figure C-1). There are many reasons to explain why model performance exhibited such a large inter-annual variability. Foremost among these is variations in the accuracy of the precipitation forcing data, a deficiency noted by in the NLDAS documentation (Cosgrove et al., 2002). Additional error was likely introduced in the downscaling of precipitation data by the Micro-Met sub-module which was required to interpolate precipitation from 13 km² to 250 m², a distance over which precipitation can change greatly in regions of large topographic relief.

Some degree of inaccuracy was anticipated in the precipitation field for a number of reasons, the most obvious being the lack of precipitation observations due to the remote and undeveloped nature inherent to the central Rocky Mountains. Radar based estimates also suffer in the rugged topography of the region, which when combined with the highly variable spatial distribution across steep elevation gradients leads to a great deal of uncertainty in the precipitation analysis; however, many of the same issues would plague station observations without the added benefit of a high temporal resolution.

SWE Validation

Validation of model derived SWE values was less than for the precipitation validation, with the model drastically under-estimating SWE accumulations across the entire domain, with substantial variability in validation from year-to-year (Figure C-2). Correlation coefficients show a moderate relationship between the simulations and observations, indicating that snow accumulates approximately at the same time in the model as it did in the real world. The net

result of this error is to shorten the snow season and reduce the snow covered area compared to the real world case.

SWE was expected to validate somewhat worse than for the precipitation due to the highly variable nature of snow accumulation over very small scales. Model values of SWE are an average depth over the entire 250 m² grid cell while observation SWE values only consider snow accumulation over a few square meters of the snow pillow, and are thus expected to not be a perfect point of comparison.

Another factor that likely contributes to this poor snow-pack representation is the model's inability to properly distinguish between liquid and solid precipitation types at temperatures near freezing. SnowModel defines the transition between rain and snow when the air temperature is below 2 °C; however, the near surface air temperature may not be representative of temperatures immediately above the near surface layer, and would likely result in snow falling when the analyzed 2 meter temperature was above 2 °C. Incorrect parameterization of precipitation phase would also influence the overall snowpack energy balance and lead to different partitions of energy fluxes associated with melting and snow cold content.

The large underestimation of snowpack distribution and depth likely means that the domain total values for sublimation are significantly underestimated. Furthermore, the large variation in model performance between years also means that comparisons of the relative magnitude of inter-annual variability in sublimation amounts are also less valid, as some years would have more snow cover, and thus comparatively larger sublimation amounts. This would also be true for the magnitudes of the daily sublimation shown in Figure 3.3; however, the annual cycle should remain representative of the effect the meteorological conditions would have on

sublimation have at different times of the year. Fortunately the high/low bias of precipitation and SWE for a given SNOTEL location appears to be the same from year to year, indicating that the results are affected in a consistent manner throughout the study period.

While the failure of the simulations to accurately represent snow accumulation in this case is a significant drawback of the simulations, there are still many important relationships that remain valid. For example, the amount of snow and snow covered area will not influence the results of sublimation across elevation or the calculated average daily sublimation rate because they are primarily driven by energy fluxes controlled by ambient meteorological conditions, and would be almost the same if there was 1mm or 1 m of snow on the ground. Comparisons between the LAI sensitivity run and the control year should also remain valid, as both simulations would experience the same amount of error in snowpack evolution with the only difference being the partitioning of snow storage and sublimation.

CHAPTER 5 : CONCLUSIONS

Sublimation and subsequent removal of water from wintertime snow cover is a major component of the water balance for any area, and results from this study demonstrate that the magnitude and character of sublimation vary considerably across a large mountain catchment. The 10 years of snowpack simulation was carried out using the best available forcing data to quantify the change in annual sublimation magnitude. In addition, the model was run at a fine grid resolution of 250 m in order to determine the spatial characteristics of sublimation. Results from this effort indicate that the amount of sublimation varies greatly from year to year depending on precipitation amount, land cover characteristics and meteorological conditions.

Results also show significant variability in sublimation rates across gradients of elevation, with high altitude areas experiencing larger rates of sublimation due to increased wind ventilation, intense solar radiation and large vapor pressure deficits. These high sublimation rates combined with the long duration of snow cover at high elevations leads to these areas having the largest total sublimation of any location within the domain.

Any numerical simulation is susceptible to errors brought about by the failure to accurately represent the actual physical phenomenon which control the energy and mass balance of a system. These errors can result from inaccurate forcing data, misrepresentations of surface topography and land cover or parameterizations of non-linear relationships. In an attempt to acknowledge some of these deficiencies secondary runs of the model were made to test the sensitivity of the model to changes in forest LAI, with a noticeable change in the fraction of sublimation.

Based on the results of this study, the author concludes that

1. Sublimation is a major component of the water balance within the UCRB, and results in a significant loss of snowpack water
2. Sublimation generally increases at higher elevations, with a sharp increase in sublimation above 3500 m MSL
3. Model derived sublimation is most efficient when snow is blowing or saltating
4. The magnitude of sublimation varies greatly on inter-annual timescales
5. On daily time scales, sublimation appears periodic in nature, with 'events' of enhanced sublimation resulting substantial loss of water from the snowpack

Furthermore, these sublimation events are driven by periods of extremely dry, and most importantly windy, conditions that are sustained for several hours or a few days.

Future Considerations

The results from this study offer many new questions about the nature of sublimation and the processes that control snow pack evolution in general. Of particular interest is the response of sublimation to changes to the forest canopy in conjunction with the ongoing bark beetle infestation. The resulting net decrease in over-all sublimation found in the sensitivity run illustrates that even subtle differences in the land surface can have profound implications on the water balance. This investigation only considered short term effects of tree mortality, namely the reduction of LAI due to needle loss; however, the future forests of the UCRB will likely see even more drastic changes as dead trees begin to fall allowing for a much different make-up of stem heights, tree species and ground cover.

Another issue that was encountered during the study was the limited computational resources available, both in terms of processing power and storage capacity. Lack of available computing power severely limited the extent to which the simulations could be carried out in terms of spatial resolution and frequency of output data. This was due in part to the large area covered by the domain which did allow for more regional and elevation-gradient inferences, but resulted in much longer computation times and excessive data issues. The selected grid size of 250 m is at the upper limit of SnowModel's ability to compute blowing snow processes, and further downscaling would allow for explicit representation these processes occurring on scales of 10's of meters.

Finally, while the NLDAS data used to force the simulations is believed to be the best for use over such a large domain, the relatively poor performance of the model in accurately simulating both precipitation amount and especially SWE amount shows that precipitation fields could be improved. In addition to improving precipitation estimation, more work needs to be done on how precipitation phase is determined. A number of relationships between air temperature and precipitation phase have been developed for the environment of the UCRB, and it would be of interest to see how altering this parameter changes the calculated values of sublimation.

If this study were to be carried out again, it should be done in a manner that puts less emphasis on spatial extent in order to focus more on small scale processes, such as vegetation snow holding capacity as it relates to canopy sublimation, that hold the most influence over sublimation. These considerations should include

1. Most accurate representation of land cover type possible, including explicitly simulating vegetation processes such as wind unloading
2. Increased resolution to capture fine scale blowing snow processes
3. Improved representation of snow cover, particularly focused on using better precipitation forcing

REFERENCES

- Beaty, C. B., 1975. Sublimation or melting: Observations from the White Mountains, California and Nevada, U.S.A., *J. Glaciol.*, Vol. 14, pp. 275-286.
- Bowling, L. C., Pomeroy, J. W., and Lettenmaier, D. P., 2004. Parameterization of Blowing-Snow sublimation in a macroscale hydrology model. *Journal of Hydrometeorology*. Vol. 5, pp.745-762.
- Bureau of Reclamation, 2012. Upper Colorado River Basin consumptive uses and losses report 2006-2010. U. S. Department of the Interior Technical Report.
- Carroll, T., Cline, D., Olheiser, C., Rost, A., Nilsson, A., Fall, G., Bovitz, C., and Li, L., 2006. NOAA's National Snow Analyses. Conference Proceedings of the 74th Annual Western Snow Conference. Las Cruces, NM.
- Christensen, N.S., and Lettenmaier, D.P., 2007. A multi-model ensemble approach to assessment of climate change impacts on the hydrology and water resources of the Colorado River Basin, *Hydrol. Earth Sys. Sci.*, 11(4): 1417-1434.
- Déry, S.J., Taylor, P.A., and Xiao, J., 1998. The thermodynamic effects of sublimating, Blowing snow in the atmospheric boundary layer. *Boundary-Layer Meteorology*. Vol. 89, pp. 251-283.
- Déry, S.J., and Yao, M.K., 1999. A bulk blowing snow model. *Boundary-Layer Meteorology*. Vol. 93. pp. 237-251.

- Fassnacht, S.R., 2004. Estimating Alter-shielded gauge snowfall undercatch, snowpack sublimation, and blowing snow transport at six sites in the coterminous USA. *Hydrol. Process.* Vol. 18, pp. 3481–3492.
- Fassnacht, S.R., 2010. Temporal changes in small scale snowpack surface roughness length for sublimation estimates in hydrological modeling. *Journal of Geographical Research*, 36(1), 43-57.
- Fry, J., Xian, G., Jin, S., Dewitz, J., Homer, C., Yang, L., Barnes, C., Herold, N., and Wickham, J., 2011. Completion of the 2006 National Land Cover Database for the Conterminous United States, *PE&RS*, Vol. 77(9):858-864.
- Gesch, D., Evans, G., Mauck, J., Hutchinson, J., Carswell Jr., W.J., 2009. The National Map—Elevation: U.S. Geological Survey Fact Sheet 2009-3053, 4 p.
- Harding, R. J., and Pomeroy, J.W., 1996. the Energy Balance of the Winter Boreal Landscape. *Journal of Climate*. Vol. 9, pp. 2778-2787.
- Hiemstra, C.A. , Liston, G.E. and Reiners, W.A., 2002. Snow Redistribution by wind and interactions with vegetation at upper treeline in the medicine bow mountains, Wyoming, USA. *Arctic, Antarctic and Alpine Research*, Vol. 34, No. 3, pp. 262-273.
- Hood, E., Williams, M., and Cline, D., 1999. Sublimation from a seasonal snowpack at a continental, mid-latitude alpine site. *Hydrological Processes*, Vol. 13, pp. 1781-1797.
- Kattelman, R., and Elder, K., 1991. Hydrologic Characteristics and water balance of an alpine basin in the Sierra Nevada. *Water Resources Research*, Vol. 27, No. 7, pp. 1553-1562.

- Liston, G. E., 1995. Local advection of momentum, heat and moisture during the melt of patchy snow covers. *Journal of Applied Meteorology*. Vol. 34, No. 7, pp. 1705-1715.
- Liston, G. E., and Hall, D. K., 1995. An energy balance model of lake ice evolution. *J. Glaciol.*, 41, 373-382.
- Liston, G. E. and Sturm, M., 1998. A snow-transport model for complex terrain. *Journal of Glaciology*. Vol. 44, No. 148, pp. 498-516.
- Liston, G. E. and Sturm, M., 2002. Winter precipitation patterns in arctic Alaska determined from a blowing-snow model and snow-depth observations. *Journal of Hydrometeorology*. Vol. 3, No. 6, pp. 646-659.
- Liston, G. E., and Elder, K., 2006. A meteorological distribution system for high-resolution terrestrial modeling (MicroMet). *Journal of Hydrometeorology*. Vol. 7, No. 2, pp. 217-234.
- Liston, G. E., and Elder, K., 2006. A distributed snow-evolution modeling system (SnowModel). *Journal of Hydrometeorology*. Vol. 7, No. 6, pp. 1259-1276.
- Liston, G. E., Haehnel, R. B., Sturm, M., Hiemstra, C. A., Berezovskaya, S., and Tabler, R. D., 2007. Simulating complex snow distributions in windy environments using SnowTran-3D. *Journal of Glaciology*. Vol. 53, No. 181, pp. 241-256.
- Liston, G. E., Hiemstra, C. A., Elder, K., Cline, D. W., 2007. Mesocell study area snow distributions for the cold land processes experiment (CLPX). *J. of Hydromet.*, Vol. 9, pp. 957-976.

- Liston, G. E. and Hiemstra, C.A., 2008. A simple data assimilation system for complex snow distributions (SnowAssim). *Journal of Hydrometeorology*. Vol. 5, No. 6, pp. 989-1004.
- MacDonald, M. K., Pomeroy, J. W., and Pietroniro, A., 2010. On the importance of sublimation to an alpine snow mass balance in the Canadian Rocky Mountains. *Hydrol. Earth Syst. Sci.*, Vol. 14, pp. 1401–1415.
- Marks, D., Dozier, J., and Davis, R. E., 1992. Climate and energy exchange at the snow surface in the alpine region of the Sierra Nevada, 1, Meteorological measurements and monitoring, *Water Resour. Res.*, Vol 28. No. 11. pp. 3043-3054.
- Marks, D., Domingo, J., Susong, D., Link, T., and Garin, D., 1999. A spatially distributed energy balance snowmelt model for application in mountain basins.
- Martinelli M., 1960. Moisture exchange between the atmosphere and alpine snow surfaces under summer conditions. *Journal of Meteorology* 17: 227-231.
- Meiman J. R., Grant L. O., 1974. Snow-air interactions and management on mountain watershed snowpack. In Environmental Research Center, Colorado State University: Ft. Collins, Colorado.
- Mesinger, F., DiMego, G., Kalnay, E., Mitchel, K., Shafran, P. C., Ebisuzaki, W., Jovic, D., Woollen, J., Rogers, E., Berbery, E. H., Ek, M. B., Fan, Y., Grumbine, R., Higgins, W., Li, H., Lin, Y., Manikin, G., Parrish, D. and Shi, W., 2006. North American Regional Reanalysis. *Bull. Amer. Meteo. Soc.*, 87, 343-360.
- Mitchell, K. E., Lohmann, D., Houser, P. R., Wood, E. F., Schaake, J. C., Robock, A., Cosgrove, B. A., Sheffield, J., Duan, Q., Luo, L., Higgins, R. W., Pinker, R. T., Tarpley, J. D.,

- Lettenmaier, D. P., Marshall, C. H., Entin, J. K., Pan, M., Shi, W., Koren, V., Meng, J., Ramsay, B., H., Bailey, A. A., 2004. The multi-institution North American Land Data Assimilation System (NLDAS): Utilizing multiple GCIP products and partners in a continental distributed hydrological modeling system. *J. of Geophysical Research*. Vol. 109, pp. 1-32.
- Molotch, N.P., Blanken, D. P., Williams, M. W., Turnipseed, A. A., Monson, R. K., and Margulis, S.A., 2007. Estimating sublimation of intercepted and sub-canopy snow using eddy covariance systems. *Hydrol. Process*. Vol. 21, pp. 1567-1575.
- Montesi, J., Elder, K., Schmidt, R. A., and Davis, R.E., 2004. Sublimation of intercepted snow within a subalpine forest canopy at two elevations. *J. Hydrometeor*, Vol. 5, 763–773.
- Neumann, T. A., Albert, M. R., Engel, C., Courville, Z., and Perron, F., 2009. Sublimation and the mass-transfer coefficient for snow sublimation. *International Journal of Heat and Mass Transfer*, Vol. 52, pp. 309-315.
- Pomeroy, J. W., 1991. Transport and sublimation of snow in wind-scoured alpine terrain. *Snow, Hydrology and Forests in High Alpine Areas (Proceedings of the Vienna Symposium, August 1991)*. IAHS Publ. no. 205.
- Pomeroy, J. W., Gray, D. M., and Landine, P. G., 1993. The prairie blowing snow model: characteristics, validation, operation. *J. Hydrol.*, Vol. 144, pp. 165-192.
- Pugh, E. T., Gordon, E. S., 2012. A conceptual model of water yield effects from beetle-induced tree death in snow-dominated lodgepole pine forests. *Hydrological Processes*. DOI: 10.1002/hyp.9312

- Schmidt, R. A., 1972. Sublimation of wind-transported snow-A Model, Res. Pap, RM-90, Rocky Mt. For. and Range Expr. Sta., For. Serv., U.S. Dept. of Agric., Fort Collins, Colo. Expr. Sta., For. Serv., U.S. Dept. of Agric., Fort Collins, Colo.
- Schmidt, R. A., Troendle, C. A., and Meiman, J. R., 1998. Sublimation of snowpacks in subalpine conifer forests. *Can. J. For. Res.*, Vol. 28, pp. 501-513.
- Schultz, O., and de Jong, C., 2004. Snowmelt and sublimation: field experiment and modeling in the high Atlas mountains of Morocco, *Journal of Hydrology & Earth Systems Science.*, Vol. 8, pp. 1076-1089.
- Strasser, U., Bernhardt, M., Weber, M., Liston, G. E. and Mauser, W., 2008. Is snow sublimation important in the alpine water balance? *The Cryosphere*, Vol. 2, pp. 53-66.
- Thorpe, A. and Mason, B., 1966. The evaporation of ice spheres and ice crystals. *British Journal of Applied Physics*, Vol. 17, pp. 541-548.
- Winstral, A., and Marks, D., 2002. Simulating wind fields and snow redistribution using terrain-based parameters to model snow accumulation and melt over a semi-arid mountain catchment. 59th Eastern Snow Conference, Stowe, Vermont.
- Zhang, Y., Suzuki, K., Kadota, T., and Ohata, T., 2004. Sublimation from snow surface in southern mountain taiga of eastern Siberia. *Journal of Geophysical Research*, Vol. 109, D21103, doi:10.1029/2003JD003779.

APPENDIX A

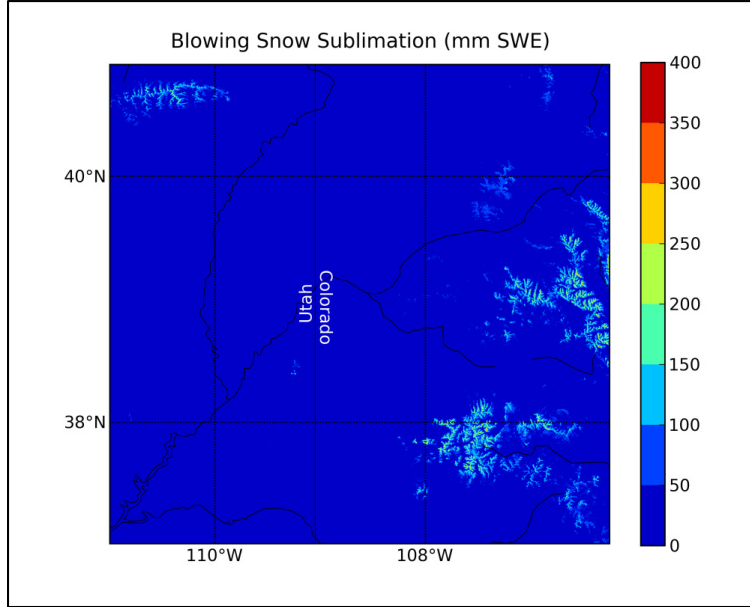


Figure A-1: Average annual simulated blowing snow sublimation from October 1, 2001 through September 30, 2011

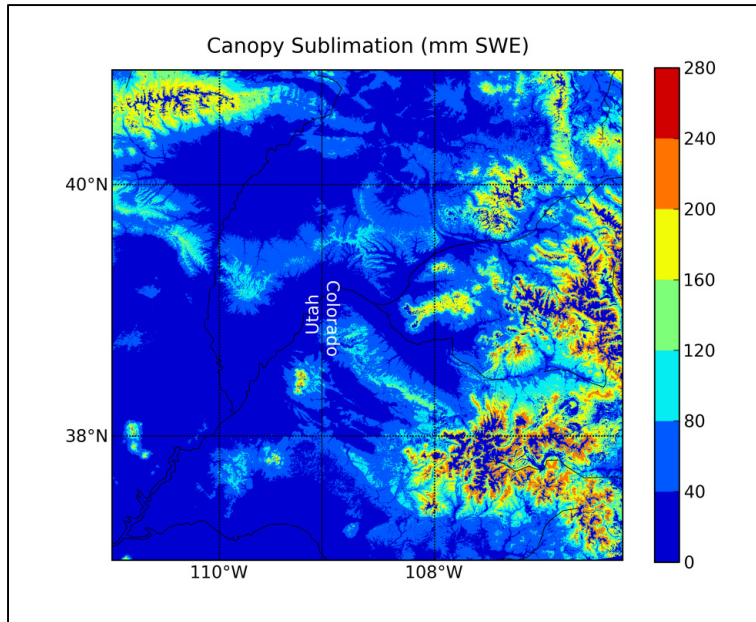


Figure A-2: Average annual simulated canopy sublimation from October 1, 2001 through September 30, 2011

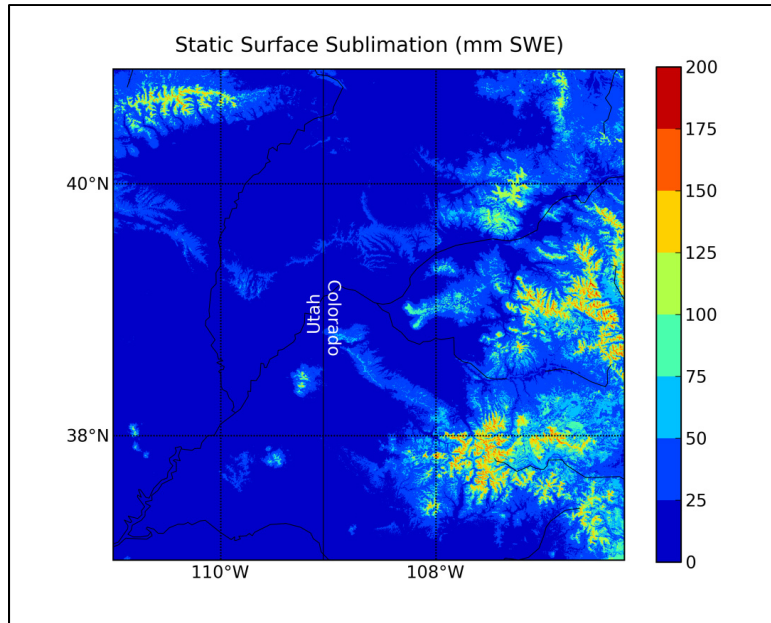


Figure A-3: Average annual simulated static surface sublimation from October 1, 2001 through September 30, 2011

APPENDIX B

Table B-1: Equivalent land type classification for the National Land Cover Dataset and land cover types found in SnowModel

	NLCD
Urban	21
	22
	23
	24
Bare	31
Deciduous Forest	41
Evergreen Forest	42
Mixed Forest	43
Shrub/scrub	52
Grass	71
Pasture	81
Cultivated	82
Wetlands	90

	SnowModel
Urban	21
	21
	21
	21
Bare	18
Deciduous Forrest	2
Evergreen Forest	1
Mixed Forest	3
Short Conifer	4
Grass	12
Pasture	23
Tall Crops	22
Wetland	9

APPENDIX C

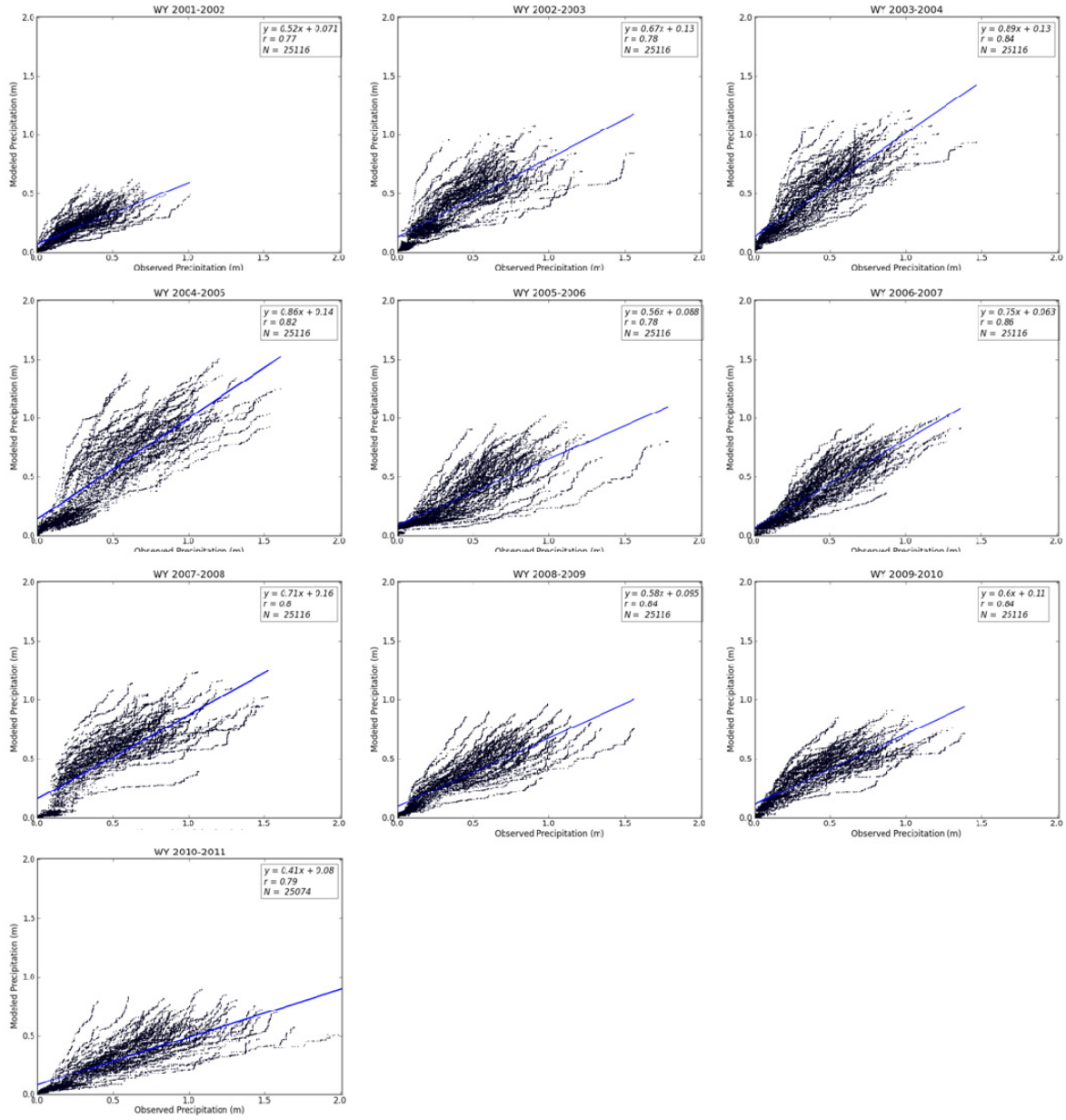


Figure C-1: Comparison of model derived precipitation to observations at 69 select SNOTEL sites

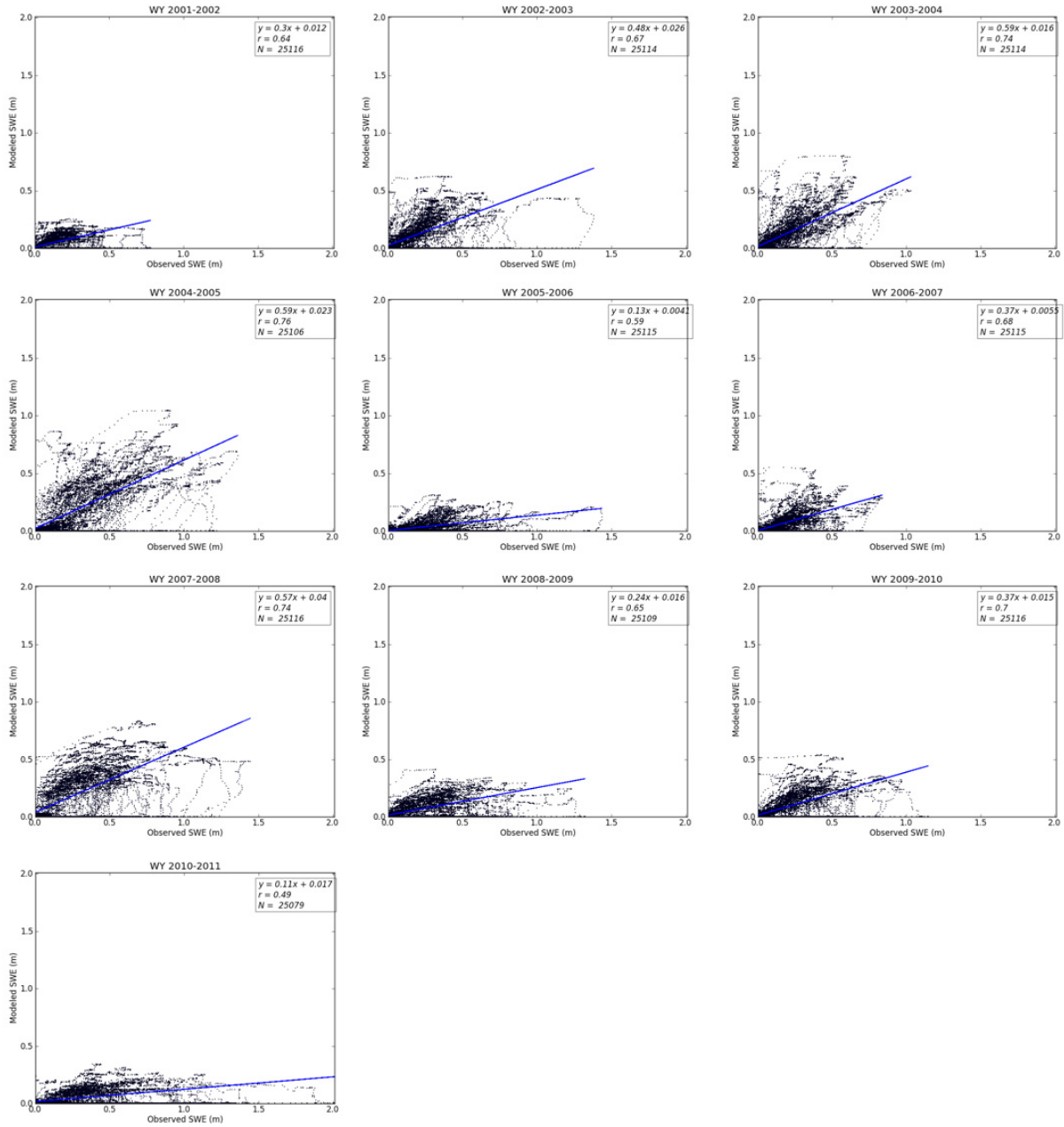


Figure C-2: Comparison of model derived SWE values to observations at 69 select SNOTEL sites